

## Response to Reviewer/Referee #1

Major comments:

1) Assess uncertainty if following today's existing SOP: While this study clearly shows the utility of single- and multi-point calibrations in these three coastal systems, it would be useful to discuss the uncertainty observed when following the existing SeaFET standard operating procedure (SOP). I believe the SOP described by Bresnahan et al. 2014 is to use the factory calibration, but correct the dataset to some independent measure of "true" pH (e.g., discrete bottle samples, pH derived from other biogeochemical sensors combined with locally-constrained carbon system algorithm or TA-S relationship) once the SeaFET has conditioned to the environment in which it is deployed. This, along with an explanation of why the Miller et al. results differ from Bresnahan et al., would be a useful analysis for the existing users of SeaFETs.

### *Response*

**Specific to Bresnahan et al. (2014), a single-point *in situ* calibration was performed after the sensor was conditioned. This is different than the factory calibration performed by Sea-Bird. Factory calibration by Sea-Bird is conducted in a highly controlled tank setting void of natural conditions.**

**We agree with the reviewer that the current SOP described by Bresnahan et al. (2014) is slightly unclear as multiple cross-reference methods are proposed when determining SeaFET<sup>TM</sup> uncertainty (e.g., discrete bottle samples, pH estimated from O<sub>2</sub> or PCO<sub>2</sub>). Thus, uncertainty will vary depending on validating source. We recognize the reviewer's comment regarding the utility of further comparing our uncertainty with that of Bresnahan et al. (2014), and have amended the manuscript to reflect this. See lines 677 - 687 in revised manuscript. Further, we refer the reviewer to lines 618- 636 which detail our assessment as to why some of our findings differ from what is currently in the primary literature.**

**We believe one utility of this manuscript is adding clarity to some of the ambiguity in terms and methods used in the primary literature regarding SeaFET<sup>TM</sup> operation and, thus, thank the reviewer for pointing out how we can improve by providing direct comparisons.**

2) Characterize environmental variability: While the authors include a thorough explanation of how they minimized the impact of time/space sampling mismatch between the SeaFETs and the various independent validation measurements, it would be useful to develop an estimate of the environmental variability within these time/space constraints. This should be subtracted from (or considered somehow in) the sensor uncertainty estimates. An example of this type of assessment of how environmental variability impacts sensor field evaluations is summarized in the following and its associated ACT pCO<sub>2</sub> sensor reports: Tamburri et al., 2011: Alliance for Coastal Technologies: Advancing Moored pCO<sub>2</sub> Instruments in Coastal Waters. Marine Technology Society Journal, 45, 43-51.

*Response*

**We agree with the reviewer that providing these estimates is beneficial. We have amended the manuscript to incorporate how rapid changes in salinity and temperature can affect pH measurements. However, this was done based on our data, and we caution operators that our deployment sites are not representative of different regions.**

**In addition, we chose to forgo adding an additional figure or amending figure 10 because environmental variability is specific to an operator's location and not specifically an intrinsic uncertainty with the SeaFET™. For this reason, we feel a detailed description of environmental variability in the text (see lines 638 -654) responding to the potential uncertainties that could arise from the effects of rapid environmental variability are sufficient.**

Minor comments/edits:

Line 124: Elaborate; what does non-controlled source water conditions mean?

*Response*

**We have elaborated this line to be clearer. Non-controlled source water refers to non-manipulated seawater.**

Line 437: State the impact of 0.21 C discrepancy on pH.

*Response*

**This line has been amended to express the uncertainty from this temperature discrepancy.**

Lines 472-474: Improved accuracy for the unconditioned vs conditioned calibration based on what? The inter-sensor anomaly seems to be less in Fig 5 (conditioned) compared to Fig 4 (unconditioned), which is also shown in Fig 6.

*Response*

**We agree with the reviewer that this may have been a bit unclear. We have amended the manuscript (see lines 481 - 482) to state the accuracy improved relative to the discrete reference samples. The reviewer is correct, the inter-sensor variability is less when calibrated and compared after the sensors were conditioned. When we discuss accuracy, we are specifically referring to sensor pH vs. discrete reference samples. We have provided a table based on reviewer # 2's comments to make clear the terminology used throughout the manuscript is consistent and clear.**

Lines 680-683: While spectral analysis is a powerful tool for identifying drivers that are periodic or regular in nature, it will not characterize many phenomenon in the coastal environment such

as storms or biological productivity/respiration. These types of events may impact the range over which a multi-point calibration should be made. This caveat should be included when suggesting spectral analysis as a tool for developing a multi-point calibration scheme in an environment with stochastic events.

***Response***

**We agree with the reviewer that spectral analysis—while useful in some systems—may not be as insightful in indicating the main drivers of pH. However, if no observable pattern is distinguishable using spectral analysis, this in itself, will help indicate which calibration method is appropriate (e.g., *in situ* single-point or multi-point).**

**We have amended the manuscript to reflect this comment according to the reviewer’s concern. Please see lines 733 – 738 in the revised manuscript.**

Line 687: Define M2.

***Response***

**We have removed the M2 term and simply stated “mixed semi-diurnal.”**

Figure 3: The temperature difference here could be misleading to the reader. It is important to be transparent by stating in the caption that the SeaFET was not fully submerged in the tank, making it susceptible to air temperature fluctuations unlike the BoL, which was measuring only tank water temperature.

***Response***

**We appreciate this comment, and have amended the figure caption to make clear that the top portion of the sensor may have been exposed to air temperature fluctuations.**

Response to Reviewer/Referee #2

Specific comments Several methods of assessing data quality have been used – variability, accuracy (= integrated uncertainty), uncertainty, “true pHt”, variance, RMSE, Standard deviation of duplicate samples, mean anomaly . . . Although Section 2.5.1 and 3.5 describes some of these terms in some detail, I found it difficult to assess the performance of the instruments and was distracted by the variety of terms. The sentence starting line 576 is a good example of this “. . . can provide and accurate measurement of pHt. . . executed with high precision.”

I suggest a table defining how and in what circumstance each term is used.

***Response***

**We thank the reviewer for the comment and have added a table defining some of the terminology used.**

Line 257 specify austral winter

*Response*

**We have amended this line to indicate winter in the northern hemisphere: boreal winter.**

Lines 343, 400 why are the calibration coefficients on the header file and the CD-ROM different? If they are different how can the correct one be verified?

*Response*

**After speaking with the engineers at Sea-Bird, I was instructed that the calibration coefficient on the CD-ROM was correct and the one written to the header file was not. After this conversation, I do not know their actions to resolve this issue, but they are aware of the problem. While I was instructed that the CD-ROM calibration coefficient is correct, we are hesitant to fully trust this response until they provide a more detailed response regarding this issue.**

Line 410 SeaFET397 emerged from the tank for 24 hours. Did the pH sensor dry out? And if so, how was it reconditioned.

*Response*

**It is not clear whether or not the electrodes dried out as the tank refilled before proper examination. Given the humidity in the room and in the tank, as well as a robust performance throughout the deployment, we do not believe the sensor was damaged. Since this failure occurred on April 8<sup>th</sup> and calibration did not occur until April 25<sup>th</sup>, any reconditioning required would have taken place within that 16 day window once the tank was refilled.**

Line 467, the absolute difference of 2.83 C is large in this context. How did you decide what temperature to use. Do you have a recommendation around calibration of the SeaFET temperature sensor?

*Response*

**We agree with the reviewer that this is a large temperature difference; however, we had more confidence in the Thermosalinograph readings given the history of reliability of this sensor in the community and at this specific location coupled to the BoL. In addition, there were multiple temperature probes monitoring incoming water throughout the hatchery that we cross-referenced. Suggestions as to accurately monitor temperature when calibrating the SeaFET<sup>TM</sup> are suggested in the manuscript. Please see lines 693 – 699.**

Line 497 How was duration of the conditioning period determined, ie the width of the blue box in Figure 6. The 14 days indicated in Figure 6 is a long time

***Response***

**Given that Bresnahan et al. (2014) indicate an approximate conditioning period of around 10 days, we were able to use this as a baseline to see when measurements stabilized over a several day period. This is how we were able to determine the conditioning period.**

Line 512 the sentence starting “There was no clear distinction in greater accuracy..” does not make sense to me. Please rewrite this.

***Response***

**This sentence has been rewritten for clarity based on the reviewer’s comment.**

Line 632 The sentence starting “For instances of . . .” makes no sense, please reword.

***Response***

**We have rewritten the sentence to be clearer. Specifically, this sentence refers to the variance within discrete reference sample collection. That is, when collecting calibration samples, replicates will display a certain degree of variance for a “true pH” value, and this should be considered when calibrating the sensor. For example, we found a higher than desired discrepancy in our triplicate calibration samples taken for Kasitsna bay, so one replicate was thrown out, and duplicate calibration samples were used rather than triplicate for calculation of a “true pH.”**

Line 648 You state that “. . .the potential uncertainties calculated in this study represent the upper limit of an average uncertainty. . .” How are you able to ascertain that this is an upper limit?

***Response***

**We suggest that these are upper limits since our ranges of uncertainty fall within and, are, greater than what previous published results have found.**

Line 654 You begin to discuss the effects of errors in the temperature measurement, but stop short of making any recommendations. This section should be tightened up, to go beyond a description of your own deployments.

***Response***

**We appreciate the reviewer's concern, but believe that there is a clear recommendation regarding temperature. We state that it would be preferable to record temperature with a more robust instrument, or track temperature before deployment and apply an offset to the thermistor value.**

Line 667 “. . .expanding the scope of pH variability. . .” this does not make sense

*Response*

**This sentence has been rewritten based on the reviewer's comment.**

It would be useful to include a bullet pointed list of recommendations in the Conclusion

*Response*

**While we agree that this may be beneficial, we feel the main objective of this manuscript is to serve as an evaluation rather than a suggested best practices as this has already been done: Bresnahan et al. 2014 and Rivest et al. 2016.**

Was there any evidence of biofouling affecting the pH measurement during any of the deployments? Would you be able to determine the effect of this with your calibration strategy, and do you have any recommendations on how to identify this problem?

*Response*

**There was no evidence of biofouling affecting any of the SeaFETs. There was no evidence of biofouling at all for the Alaska SeaFETs, and the one at sentry shoal underwent maintenance during its deployment. In addition, this sensor appeared to provide the most accurate measurements.**

**As far as identifying biofouling as interference, we do not offer suggestions, but this should be identifiable when you start to see a consistent drift in readings. This can be compared against other oceanographic data and the other electrode to verify biofouling, as well as a close physical inspection upon recovery. At the time biofouling is identified, calibration will need to be redone once the sensor is cleaned.**

References – These are complete and up to date.

*Response*

**No reply needed.**

Figures – In general these are clear and helpful. I do not understand, however, the difference between Figure 4 and Figure 5. They are the same data sets, but Figure 4 is for “before they were conditioned”, and “Figure 5 is for ‘conditioned’”. Does this refer to the way they were calibrated? Please clarify in the Figure caption.

*Response*

**The reviewer is correct, this does refer to how they were calibrated. We have amended the caption in figure 5 to make this clear.**

1 An Evaluation of the Performance of Sea-Bird Scientific's Autonomous SeaFET™:  
2 Considerations for the Broader Oceanographic Community

3  
4 Cale A. Miller<sup>1,3</sup>, Katie Pocock<sup>2</sup>, Wiley Evans<sup>2</sup>, and Amanda L. Kelley<sup>1\*</sup>

5  
6 1. College of Fisheries and Ocean Sciences, University of Alaska Fairbanks, Fairbanks, AK,  
7 USA

8  
9 2. Hakai Institute, Heriot Bay, BC, Canada

10  
11 3. **Present address:** Department of Evolution and Ecology, College of Biological Sciences,  
12 University of California Davis, CA, USA

13  
14 \*Correspondence to: Amanda L. Kelley (alkelley@alaska.edu)

15  
16  
17 **Abstract**

18  
19 The commercially available Sea-Bird SeaFET™ provides an accessible way for a broad  
20 community of researchers to study ocean acidification and obtain robust measurements of  
21 seawater pH via the use of an *in situ* autonomous sensor. There are pitfalls, however, that have  
22 been detailed in previous best practices for sensor care, deployment, and data handling. Here, we  
23 took advantage of two distinctly different coastal settings to evaluate the Sea-Bird SeaFET™ and  
24 examine the multitude of scenarios in which problems may arise confounding the accuracy of  
25 measured pH. High-resolution temporal measurements of pH were obtained during 3- to 5-month  
26 field deployments in three separate locations (two in south-central, Alaska, USA, and one British  
27 Columbia, Canada) spanning a broad range of nearshore temperature and salinity conditions.  
28 Both the internal and external electrodes onboard the SeaFET™ were evaluated against robust  
29 benchtop measurements for accuracy utilizing either the factory calibration, an *in situ* single-  
30 point calibration, or *in situ* multi-point calibration. In addition, two sensors deployed in parallel  
31 in Kasitsna Bay, AK, USA, were compared for inter-sensor variability in order to quantify other  
32 factors contributing to SeaFET™ intrinsic inaccuracies. Based on our results, the multi-point  
33 calibration method provided the highest accuracy (< 0.025 difference in pH) of pH when  
34 compared against benchtop measurements. Spectral analysis of time series data showed that  
35 during spring in Alaskan waters, a range of tidal frequencies dominated pH variability, while  
36 seasonal oceanographic conditions were the dominant driver in Canadian waters. Further, it is  
37 suggested that spectral analysis performed on initial deployments may be able to act as an *a*  
38 *posteriori* method to better identify appropriate calibration regimes. Based on this evaluation, we  
39 provide a comprehensive assessment of the potential sources of uncertainty associated with  
40 accuracy and precision of the SeaFETs™ electrodes.

41  
42 **1 Introduction**

43  
44 The intrusion of excess anthropogenic CO<sub>2</sub> into the global oceans—referred to as ocean  
45 acidification (OA)— induces a series of geochemical reactions that increases seawater [H<sup>+</sup>]  
46 (lowering pH) while concomitantly reducing the ocean's overall buffering capacity by reducing



47 the  $[\text{CO}_3^{2-}]$  (Caldeira and Wickett, 2003; Orr et al., 2005). Due to more dynamic natural physical  
48 and chemical processes in the coastal ocean, a differentiation exists between open-ocean  
49 acidification and nearshore coastal acidification. Open-ocean acidification of surface waters is  
50 predominately a function of equilibration with atmospheric  $p\text{CO}_2$ , thus increasing on yearly and  
51 decadal timescales as continued burning of fossil fuels ensues (Hofmann et al., 2011; Orr et al.,  
52 2005). Coastal acidification, however, can manifest on short time and space scales driven by  
53 riverine input and its chemical constituents (e.g., organic carbon, nutrients, and organic  
54 alkalinity), community metabolism and organization, tidal cycles, upwelling, and groundwater  
55 input (Duarte et al., 2013; Sunda and Cai, 2012; Waldbusser and Salisbury, 2014), all of which  
56 can act in conjunction with increasing atmospheric  $\text{CO}_2$ , leading to more frequent, intense, and  
57 longer-lasting acidification events (Hales et al., 2016; Harris et al., 2013). In the face of rapidly  
58 changing coastal conditions, tracking and quantifying the progression of OA requires precise and  
59 accurate measurements of carbonate chemistry over long periods of time; these can be achieved  
60 by appropriately constraining the carbonate system by measuring at least two of the system's  
61 parameters: total dissolved inorganic carbon ( $\text{TCO}_2$ ), total alkalinity (TA), pH, and the partial  
62 pressure of  $\text{CO}_2$  ( $p\text{CO}_2$ ). Despite the marked increase in OA research over the past decade  
63 (Riebesell and Gattuso, 2015; Rudd, 2017), nearshore monitoring efforts—particularly in  
64 estuarine waters—have been slow to ramp up, however, efforts are beginning to intensify as  
65 technological advancements are made (Feely et al., 2010, 2016; Hales et al., 2016; Harris et al.,  
66 2013; Newton et al., 2012; Waldbusser and Salisbury, 2014; Chan et al., 2017).

67  
68         Acidification of Alaskan coastal waters is predicted to progress rapidly relative to other  
69 regions within the next 50 years, and negatively impact the social-ecological structure of Alaskan  
70 marine resources by disrupting the Alaska Native subsistence and commercial fisheries (Ekstrom  
71 et al., 2015; Mathis et al., 2015b). The ocean waters present along the Alaskan coastline  
72 experience chemical and physical drivers of seawater chemistry that are unique to this region.  
73 The low seawater temperatures inherently have higher concentrations of dissolved  $\text{CO}_2$ , and  
74 chemical and physical oceanic processes unique to Alaskan waters such as sea ice melt, glacial  
75 discharge, and benthic pelagic coupling across shallow shelves are likely to exacerbate  
76 acidification in this region (Evans et al., 2014; Mathis et al., 2011a, 2011b, 2012). Recently, an  
77 OA monitoring initiative has been setup by the Alaska Ocean Observing Network (AOOS) to  
78 track and provide accessible material dedicated to acidification research in Alaskan waters  
79 (<http://www.aoos.org/alaska-ocean-acidification-network>). Along the Pacific coast of Alaska, a  
80 robust benchtop system known as a Burke-o-Lator (BoL), which measures  $\text{TCO}_2$  and  $p\text{CO}_2$   
81 either continuously in a flow-through environment or from discrete seawater samples (Bandstra  
82 et al., 2006; Barton et al., 2012; Hales et al., 2016) has been installed in several locations,  
83 including the OceansAlaska Shellfish Hatchery in Ketchikan, the Alutiiq Pride Shellfish  
84 Hatchery in Seward (Evans et al., 2015), and at the Sitka Tribe of Alaska Environmental  
85 Research Center (real-time data from Alaskan and other BoLs:  
86 [http://www.ipacoa.org/Explorer?action=oiw:fixed\\_platform](http://www.ipacoa.org/Explorer?action=oiw:fixed_platform)). Nominal analytical uncertainty for  
87  $\text{TCO}_2$  determinations from this system is 0.2% based on the reproducibility of sample and  
88 certified reference material (CRM; provided by A. Dickson analyses). For  $p\text{CO}_2$  determinations,  
89 analytical uncertainty is 1.5% based on the inaccuracy of calculated CRM alkalinity relative to  
90 the certified value. While the BoL has significant advantages for achieving robust OA  
91 measurements in nearshore waters, the physical constraints of a benchtop system limit the spatial  
92 dimension of which carbonate chemistry parameters can be measured. One potential resolution

93 to diminish the gap in coverage of OA monitoring is to utilize autonomous pH sensors, which are  
94 far more versatile in their ability to monitor hard-to-reach areas.

95  
96 Recent assessments regarding OA monitoring efforts have specifically highlighted the  
97 benefits of accessibility by the commercially produced SeaFET<sup>TM</sup> pH sensor utilizing Honeywell  
98 Durafet technology (Martz et al., 2015). The SeaFET<sup>TM</sup> was originally developed at the  
99 Monterey Bay Aquarium Research Institute (Martz et al., 2010), but since has been  
100 manufactured and distributed by Satlantic (<http://www.satlantic.com>), which is now incorporated  
101 into Sea-Bird Scientific (<http://www.seabird.com>). The partnership between MBARI, Scripps  
102 Institute of Oceanography, and Satlantic led the way for commercial availability of the  
103 SeaFET<sup>TM</sup>, providing a ready-to-deploy-factory calibration, quick start manual, and user-friendly  
104 interface. The first generation of SeaFETs<sup>TM</sup> (not distributed by Sea-Bird, but by Dr. Todd Martz  
105 at Scripps Institute of Oceanography) have been deployed in numerous field studies and were  
106 heavily scrutinized in order to provide robust best practices for appropriate calibration and  
107 deployment procedures (Bresnahan et al., 2014; Hofmann et al., 2011; Kapsenberg and  
108 Hofmann, 2016; Martz et al., 2010; Matson et al., 2011; Yu et al., 2011). More recent studies  
109 have expanded the scope of SeaFET<sup>TM</sup> accuracy, inter-sensor variability, operator experience,  
110 and multi-point calibration techniques (Gonski et al., 2018; Johnson et al., 2017; Kapsenberg et  
111 al., 2017; McLaughlin et al., 2017). Given the multitude of information regarding SeaFET<sup>TM</sup>  
112 performance, coalescing all the potential sources of uncertainty in measurements (e.g., inter-  
113 sensor variability and calibration method) can be logistically challenging for non-experienced  
114 oceanographers who now have access to the commercially available SeaFETs<sup>TM</sup> distributed by  
115 Sea-Bird.

116  
117 In this study, we aimed to take advantage of two distinct coastal settings in order to  
118 deploy and evaluate the commercially available Sea-Bird SeaFET<sup>TM</sup>, and the potential  
119 uncertainties that can arise with time series pH<sub>t</sub> (total scale) measurements. For this evaluation,  
120 SeaFETs<sup>TM</sup> were co-deployed side-by-side to quantify inter-sensor variability, discrepancies  
121 were examined between factory calibration, *in situ* single-point calibration, and *in situ* multi-  
122 point calibration pH<sub>t</sub> values, and anomalous data associated with SeaFET<sup>TM</sup> conditioning times  
123 were detailed and considered as potential sources of measurement inaccuracies. All evaluations  
124 of SeaFET<sup>TM</sup> performance were under non-controlled source water conditions (*i.e.*, **non-**  
125 **manipulated seawater**) or by *in situ* deployments. Three SeaFETs<sup>TM</sup> were deployed in coastal  
126 waters and were subjected to tidal influences and freshwater input, while a fourth was compared  
127 to pH<sub>t</sub> values derived from measurements obtained by a BoL. Finally, a spectral analysis of the  
128 quality-controlled data was performed in order to identify the driving mechanism of pH<sub>t</sub>  
129 variability between these divergent sites and consider possible un-accounted for calibration  
130 errors that could occur in dynamic settings that might not be resolved using a specific calibration  
131 method.

## 132 **2 Methods**

### 133 **2.1 Apparatus: SeaFET<sup>TM</sup>**

134  
135 The commercially available Sea-Bird SeaFET<sup>TM</sup> has retained the basic design of the original  
136 SeaFET<sup>TM</sup> developed at MBARI (Martz et al., 2010). The SeaFET<sup>TM</sup> utilizes the ion sensitive  
137

139 field effect transistor (ISFET) technology, and is outfitted with an internal Honeywell Durafet  
 140 and an external solid-state chloride selective electrode (Cl-ISE) along with an internal thermistor,  
 141 which derives temperature using the (Steinhart and Hart, 1968) equation. The internal reference  
 142 electrode is intrinsically insensitive to salinity over a tested range from 30 – 36 (Bresnahan et al.,  
 143 2014), with recent work even suggesting near-ideal Nernstian response to salinity as low as ~9.0  
 144 (Gonski et al., 2018). This is in converse to the chloride sensitive external electrode, which is  
 145 salinity dependent. Both electrodes demonstrate exceptional stability over a range of moderate  
 146 salinity (30 – 36) and broad temperature (-1 to 35 °C) (Bresnahan et al., 2014; Kapsenberg et al.,  
 147 2015; Martz et al., 2014, 2010). The range of salinity sensitivity for the external electrode has  
 148 even been extended down to 20, where it displays a near-ideal Nernst slope (Takeshita et al.,  
 149 2014). Sea-Bird suggests that the external reference electrode provides the more accurate and  
 150 stable pH<sub>i</sub> measurement given that chloride concentration can be precisely determined from  
 151 accurate salinity measurements. This is in agreement with previous research demonstrating that  
 152 the external electrode has a more robust stability (Martz et al., 2010). In dynamic nearshore  
 153 environments (e.g., estuaries with strong tidal and riverine fluxes), however, the pH<sub>i</sub> derived  
 154 from the internal electrode is recommended (Sea-Bird Scientific’s Branham, C., pers. comm.)  
 155 despite the potential of thermodynamic hysteresis (Martz et al., 2010). Bresnahan et al. (2014)  
 156 demonstrated that the internal electrode is of the highest quality and under most scenarios  
 157 remains nearly as stable as the external electrode—this was further corroborated by Gonski et al.  
 158 (2018) with SeapHOx deployments in the Murderkill estuary, Delaware.

## 159 2.2 Calibration

160  
 161 Currently, three different calibration methods are present for the SeaFET<sup>TM</sup>: a factory pre-  
 162 deployment single-point calibration, *in situ* single-point calibration, and an *in situ* multi-point  
 163 calibration (Bresnahan et al., 2014; Gonski et al., 2018). To properly calculate pH<sub>i</sub> from  
 164 SeaFET<sup>TM</sup> voltage readings, an appropriate calibration coefficient is required. The applied  
 165 calibration coefficients from the factory are a single-point, pre-deployment calibration. Given  
 166 that a conditioning period is required for the SeaFET<sup>TM</sup> (Bresnahan et al., 2014), these  
 167 coefficients are likely not adequate once the sensor becomes conditioned to the environment to  
 168 which it is deployed. For the internal electrode, the new calibration coefficient  $k_{0i}$  can be  
 169 determined as  
 170

$$171 \quad k_{0i} = -S_{Nernst} * pH_t + V_{int} - k_{2i} * T, \quad (1)$$

172 and  $k_{0e}$  for the external electrode

$$173 \quad k_{0e} = V_{ext} - pH_t + \log\left(1 + \frac{S_t}{K_s}\right) - 2 * \log(\gamma_{HCl}) - \log(Cl_T) * S_{nernst} + k_{2e} * T \quad (2)$$

174  
 175 where  $V_{FET}$  is the voltage from the electrode and  $k_2$  is the temperature coefficient ( $dE^*/dT$ )  
 176 applied to all SeaFETs<sup>TM</sup> (Martz et al., 2010). For detailed definitions of  $S_{nernst}$  and the salinity  
 177 dependent constants  $\gamma_{HCl}$  (HCl activity coefficient),  $Cl_T$  (total chloride),  $S_T$  (total sulfate), and the  
 178  $HSO_4^-$  dissociation constant  $K_s$  (Dickson et al., 2007; Khoo et al., 1977) in equations 1 and 2, we  
 179 refer readers to Martz et al. (2010), Bresnahan et al. (2014), and Sea-Bird Scientific SeaFET<sup>TM</sup>  
 180 Product Manual 2.0.0. In the literature, SeaFET<sup>TM</sup> calibration coefficients have been denoted as  
 181  $E_{int}^*$  and  $E_{ext}^*$  (Martz et al. 2010, Bresnahan et al. 2014), however, for the purpose of this

185 evaluation—which specifically examines commercially available Sea-Bird SeaFETs™—the  
186 adoption of  $k_0$  and  $k_2$  is in accordance with the preferred nomenclature from the manufacturer.  
187

188 Unlike the factory pre-deployment single-point calibration, the *in situ* single-point  
189 calibration occurs after the sensor has been deployed in the field. At the operator’s discretion, a  
190 discrete sample will be collected in direct proximity to the deployed SeaFET™ at the same time  
191 that the sensor is actively making a measurement, and then measured for  $\text{pH}_i$  at *in situ*  
192 temperature and salinity. The known  $\text{pH}_i$  would then be used in the above equations as the “ $\text{pH}_i$ ”  
193 variable. Similar to the single-point *in situ* calibration, the multi-point calibration derives a series  
194 of calibration coefficients over a short period of time that is long enough to capture environment  
195 variability such as tidal fluxes, and then a single calibration coefficient is averaged. Both single-  
196 point calibration methods—pre-deployment and *in situ*—appear to be suitable for fairly static  
197 environmental conditions, whereas the multi-point *in situ* calibration is best suited for dynamic  
198 nearshore environments (Bresnahan et al., 2014; Gonski et al., 2018).  
199

### 201 2.3 SeaFET™ conditioning: test tank deployments 202

203 A series of three separate test tank deployments for three SeaFETs™<sub>395, 396, 397</sub> were conducted in  
204 order to determine the conditioning period for each sensor. Initial sensor deployments took place  
205 in October 2016 at the Alutiiq Pride Shellfish Hatchery (APSH) in Seward, Alaska. Sensors were  
206 deployed for a duration of 72 hours in a flow-through 60 L tank where seawater taken from a  
207 depth of ~75 m in Resurrection Bay was sand-filtered, UV treated, and finally run through a 5  
208  $\mu\text{m}$  mesh. All three sensors were programmed with identical sampling settings (Table 1). The  
209 onboard internal thermistor was used to calculate temperature, and measurements of seawater  
210 salinity incoming to the hatchery were collected by a Sea-Bird Scientific SBE 45 MicroTSG  
211 Thermosalinograph that is paired with the BoL and are available on the Alaska Ocean Observing  
212 System (<http://portal.aos.org/real-time-sensors.php#map>). Factory calibration coefficients for  
213 the internal ( $k_{0i}$ ,  $k_{2i}$ ) and external ( $k_{0e}$ ,  $k_{2e}$ ) electrodes were retained when processing raw voltage  
214 data.  
215

216 A second tank deployment for the same three SeaFETs™<sub>395, 396, 397</sub> were deployed at the  
217 University of Alaska, Fairbanks, in the Ocean Acidification Research Center (OARC). Seawater  
218 collected from the APSH was delivered to the OARC test tank, ~370 L in a half-filled tank.  
219 Seawater in the tank was circulated continuously and covered to aid in the prevention of  
220 evaporation and photosynthesis. A co-deployed Sea-Bird SBE 16plusV2 SeaCAT (recently  
221 serviced by Sea-Bird) collected temperature and salinity readings every 5 minutes.  
222 SeaFETs™<sub>395, 396, 397</sub> were deployed for a duration of nine days in continuous operation mode  
223 which forgoes the ability to set frames per burst; average number of reads was identical between  
224 all sensors (Table 1). From 1 – 4 November 2016, duplicate discrete bottle samples were  
225 collected in 250 ml glass bottles with screw caps at ~00:00 and 17:00 UTC per day. Bottle  
226 samples were preserved with 20  $\mu\text{l}$  of saturated  $\text{HgCl}_2$  and processed at a later date for  $\text{TCO}_2$  and  
227 TA with a VINDTA 3C (Versatile Instrument for the Determination of total inorganic carbon  
228 and titration alkalinity). The VINDTA 3C has an uncertainty typically near 0.05% (Mathis et al.,  
229 2014, 2015a). Bottle sample  $\text{pH}_i$  was calculated using CO2SYS with known  $\text{TCO}_2$  and TA using  
230 the constants provided by (Uppström, 1974) and (Lueker et al., 2000); derived  $\text{pH}_i$  was then

231 compared against SeaFET™ sensor  $pH_t$  to test the accuracy of both internal and external  
232 electrodes, assuming the discrete bottle samples were the “true  $pH$ ” of the seawater. Upon  
233 recovery, all SeaFETs™<sup>395, 396, 397</sup> were placed into polled mode and stored with wet caps filled  
234 with tris buffer (salinity 34,  $pH$  8.09 at room temperature, 25 °C). Again, the factory calibration  
235 coefficients for the internal and external electrodes were retained when raw voltage was  
236 processed. Since the SBE 16plusV2 sampled every 5 min, salinity and temperature measured by  
237 the SBE at each 5-minute point was repeated for the following 4 minutes in order to calculate  
238 continuous minute readings by SeaFETs™<sup>395, 396, 397</sup>.

239  
240 A final test tank deployment of the SeaFETs™<sup>395, 396, 397</sup> at OARC was conducted after an  
241 assumed adequate conditioning period of nine days (first OARC deployment). All three  
242 SeaFETs™<sup>395, 396, 397</sup> had been set to polled mode after the end of the previous deployment and,  
243 therefore, were sleeping for 83 days until this final seven day deployment. The sampling settings  
244 were identical to the first OARC deployment for all three SeaFETs™<sup>395, 396, 397</sup> (Table 1). Similar  
245 to the previous OARC tank deployment, a co-deployed Sea-Bird SBE 16plusV2 SeaCAT  
246 collected temperature and salinity mirroring the SeaFET sampling interval of 3 hrs.

247  
248 The internal thermistor of each SeaFET™<sup>395, 396, 397</sup> was tested for accuracy by comparing  
249 its derived *in situ* temperature to that collected by the Sea-Bird SBE 16plusV2 during the test  
250 tank deployments. The temperature difference between the internal thermistor and the SBE  
251 16plusV2 was used to calculate the average and maximum discrepancy between the two  
252 temperature readings. The temperature discrepancy was then applied to a combination of TA:  
253  $TCO_2$  ratios over a range of salinity (20 – 35) in CO2SYS (constants: Uppström, 1974; Lueker et  
254 al., 2000), which produced two different  $pH_t$  values. The difference between these two  $pH_t$   
255 values were, therefore, concluded to be a result of the temperature discrepancy.

## 257 2.4 SeaFET™ performance: field deployments

258  
259 In late [boreal](#) winter 2017—32 days post final tank deployment—SeaFET™<sup>397</sup> was deployed at  
260 the APSH and the two remaining sensors (SeaFET™<sup>395, 396</sup>) in Kasitsna Bay within greater  
261 Kachemak Bay, Alaska (Fig. 1). At the APSH (60° 5' 55.59"N, 149° 26' 39.80"W), incoming  
262 seawater from Resurrection Bay at a depth of 75 m is split before running through a series of  
263 hatchery water filters so that an unfiltered line is run directly to the BoL. The incoming line to  
264 the BoL was then split to feed an ~11.5 L conical tank housing the SeaFET™<sup>397</sup> fit with the  
265 copper bio-fouling guard; tank residence time was ~7.5 min. The SeaFET™<sup>397</sup> at this location  
266 was deployed on 6 March 2017 with a robust sampling setting (Table 1). Two calibration  
267 methods were applied for this SeaFET™<sup>397</sup>, an *in situ* single-point calibration and an *in situ*  
268 multi-point calibration. Both calibrations were performed 50 days after deployment on 25 April  
269 2017 once the BoL had completed service maintenance. The single-point *in situ* calibration was  
270 taken during midday tide transition in Resurrection Bay, while the multi-point *in situ* approach  
271 used five (sensor sampling 3 h intervals) time points spanning an entire tidal cycle. The single-  
272 point *in situ* calibration was used to derive  $k_{0i}$  for the internal electrode (eq. 1) and  $k_{0e}$  for the  
273 external electrode (eq. 2). The multi-point *in situ* calibration followed the same formulations  
274 with the difference being the final calibration coefficient calculated was the average of the five  
275 independently calculated calibration coefficients. Three final  $pH_t$  values for the SeaFET™<sup>397</sup>  
276 were, therefore, calculated based upon the different calibration coefficients (factory, single-point

277 and multi-point *in situ* calibration) and compared against the  $pH_t$  determined from continuous  
278  $pCO_2$  measurements by the BoL and derived TA (TA-S equation, Evans et al. 2015) using  
279 CO2SYS with constants provided by Uppström (1974) and Lueker et al. (2000).  $pH_t$  uncertainty  
280 from the BoL using this combination of measured and derived parameters is 0.007 units based on  
281 propagating the error of the BoL  $pCO_2$  uncertainty reported above with the RMSE ( $17 \mu mol kg^{-1}$ )  
282 of the regional TA-S relationship (Orr, et al., *in prep*).  
283

284 Inter-sensor variability was examined between two SeaFETs<sup>TM</sup><sub>395, 396</sub> deployed off the  
285 pier at the Kasitsna Bay laboratory in Kachemak Bay ( $59^{\circ}28' 6.71''N$ ,  $151^{\circ}33'11.12''W$ ) ~1.5 m  
286 from the bottom: depth at this location fluctuates between ~7.5 – 16.8 m (Fig. 1). On 18 March  
287 2017—44 days post final tank deployment—SeaFETs<sup>TM</sup><sub>395, 396</sub> were attached to the pier piling  
288 directly beside one another on a single mooring frame. Both SeaFETs<sup>TM</sup> were wrapped with pipe  
289 tape to minimize biofouling and fit with their respective copper biofouling guards which had a  
290 tributyltin plug attached to the inside of the guard. The sampling settings for both SeaFETs<sup>TM</sup><sub>395,</sub>  
291 <sub>396</sub> were identical to the one at the APSH (Table 1). Five discrete reference samples were taken in  
292 duplicate: one sample on day of deployment (UTC: 3-18-17, 18:00), two samples 1-day post-  
293 deployment (UTC: 19 March 2017, 03:00 and 15:00), and two samples 2- and 1-day pre-  
294 recovery of the SeaFETs<sup>TM</sup><sub>395, 396</sub> (UTC 3 June 2017, 03:00; 6 June 2017, 03:00). Reference  
295 samples were collected within 30 s of the instrument sampling time period via a diver's hand  
296 Niskin, measured for temperature and salinity with a YSI 3100 conductivity instrument, stored in  
297 250 ml glass bottles with screw caps, poisoned with 100  $\mu l$  of saturated  $HgCl_2$ , and secured with  
298 teflon tape around the bottleneck threading and Parafilm wrapped on the outside of the cap.  
299 Calibration samples were processed for  $TCO_2$  and TA with a VINDTA 3C and  $pH_t$  calculated  
300 using CO2SYS with the constants provided by Uppström (1974) and Lueker et al. (2000).  
301 Salinity measurements collected by the Kachemak Bay National Estuarine Research Reserve  
302 data sonde, 10 km SE of the deployed sensors ( $59^{\circ}26' 26.87''N$ ,  $151^{\circ}43'15.21''W$ ), were used  
303 along with the SeaFET's<sup>TM</sup> internal thermistor readings to calculate  $pH_t$  from the raw voltage  
304 data in order to capture representative environmental conditions providing relevance for the  $pH_t$   
305 time series in this location. A static salinity of 32 was also used for all calculations of  $pH_t$  as an  
306 assessment of variability due to salinity measured from a data sonde 10 km away. A total of four  
307 different  $pH_t$  values for both SeaFETs<sup>TM</sup><sub>395, 396</sub> were calculated based on calibration method  
308 (factory pre-deployment single-point calibration and the *in situ* single-point) and conditioning:  
309 either conditioned or non-conditioned to the environment. All calculated  $pH_t$  values from the  
310 SeaFETs<sup>TM</sup><sub>395, 396</sub> were then compared against the remaining discrete reference bottle samples  
311 not used for calibration. This was done in order to examine the accuracy and inter-sensor  
312 variability difference between conditioned and non-conditioned to the environment electrodes.  
313 Because the Kachemak Bay data sonde was located 10 km from the deployed SeaFETs<sup>TM</sup><sub>395, 396</sub>,  
314 the measured temperature and salinity from the discrete reference samples were used to  
315 determine  $pH_t$  for the internal and external electrodes at those specific time points. That is,  
316 sensor accuracy for these two SeaFETs<sup>TM</sup><sub>395,396</sub> was only assessed with accurate temperature and  
317 salinity values determined from the discrete bottle samples.  
318

319 A fourth SeaFET<sup>TM</sup><sub>268</sub> operated by the Hakai Institute was deployed on Environment  
320 Canada's Sentry Shoal weather buoy in the Northern Strait of Georgia, BC, Canada:  $49^{\circ} 54'$   
321  $24.00''N$ ,  $124^{\circ} 59' 5.99''W$  (Fig.1). The Sentry Shoal mooring site is in a water depth of 15 m and  
322 the SeaFET<sup>TM</sup><sub>268</sub> was affixed at a depth of 1 m. A pre-deployment bucket test was conducted for

323 24 h at a sampling interval of 30 min with an average of 10 samples per frame and 30 frames per  
 324 burst from 28 – 29 June 2016. SeaFET<sup>TM</sup><sub>268</sub> was outfitted with a copper housing guard and  
 325 wrapped with copper tape. Sensor underwent two separate deployments, an initial deployment,  
 326 and a redeployment (6 July and 27 August 2016) that occurred after the sensor was retrieved for  
 327 cleaning and maintenance. Two separate calibration samples (taken in triplicate) were taken in  
 328 accordance with each deployment, and occurred 13 and 7 days after each deployment (19 July  
 329 and 2 September 2016). For each deployment, SeaFET<sup>TM</sup><sub>268</sub> settings were similar to the others at  
 330 the APSH and in Kasitsna Bay (Table 1). All calibration samples were taken in triplicate at a  
 331 depth of 1 m via CTD and Niskin bottle castings and collected in 350 ml amber glass bottles with  
 332 polyurethane-lined crimp-sealed metal caps and poisoned with 200 µl of saturated HgCl<sub>2</sub>, and  
 333 then processed for TCO<sub>2</sub> and pCO<sub>2</sub> with a BoL at the Hakai Institute’s Quadra Island Field  
 334 Station. The measured values were used to derive pH<sub>t</sub> using CO2SYS with the constants  
 335 provided by (Uppström, 1974) and (Lueker et al., 2000) in order to perform a single-point *in situ*  
 336 calibration. Uncertainty in pH determinations from BoL pCO<sub>2</sub> and TCO<sub>2</sub> measurements was  
 337 0.006 units. After SeaFET<sup>TM</sup><sub>268</sub> deployment and calibration, a total of three, triplicate, reference  
 338 sample sets were taken and processed for pH<sub>t</sub> following the procedure used for calibration  
 339 samples, then compared against SeaFET pH<sub>t</sub>.

## 340 2.5 Quantifying pH<sub>t</sub> and intrinsic sensor uncertainties

341  
 342 Calculating pH<sub>t</sub> from the SeaFET’s<sup>TM</sup> raw voltage reading is dependent on temperature, salinity  
 343 and an ideal 100% Nernstian response. The software application SeaFETcom permits the  
 344 operator to automatically calculate pH<sub>t</sub> by assigning the calibration coefficient either written to  
 345 the sensor’s header file or the one provided on the CD-ROM (these should be identical).  
 346 Determination of final pH<sub>t</sub> values from the first test tank deployment at the APSH were  
 347 calculated by two different operators and two sources for the factory pre-deployment single-point  
 348 calibration coefficients: header file and CD-ROM disc file. Aside from that exception, all other  
 349 final pH<sub>t</sub> values for the internal and external electrodes were calculated with the Mathworks  
 350 software MATLAB (V. 2016a) and Microsoft excel (v. 2016) using the following equations for  
 351 the internal electrode

$$352 \quad pH_{int} = \frac{V_{FET|INT} - k_{0i} - k_{2i} * T}{S_{nernst}}, \quad (3)$$

354 and the external electrode

$$355 \quad pH_{ext} = \frac{V_{FET|EXT} - k_{0e} - k_{2e} * T}{S_{nernst}} + \log(Cl_T) + 2 * \log(\gamma_{HCl}) - \log\left(1 + \frac{S_t}{K_s}\right) \quad (4)$$

356 where V<sub>FET</sub> is the voltage from the electrode and k<sub>2</sub> is the temperature coefficient (dE\*/dT)  
 357 applied to all SeaFETs<sup>TM</sup> (Martz et al. 2010). Again, for detailed definitions of S<sub>nernst</sub> and the  
 358 salinity dependent constants γ<sub>HCl</sub> (HCl activity coefficient), Cl<sub>T</sub> (total chloride), S<sub>T</sub> (total sulfate),  
 359 and the HSO<sub>4</sub><sup>-</sup> dissociation constant K<sub>s</sub> (Khoo et al. 1977, Dickson et al. 2007) in equations 3 and  
 360 4, we refer readers to Martz et al. (2010), Bresnahan et al. (2014), and Sea-Bird Scientific  
 361 SeaFET<sup>TM</sup> Product Manual 2.0.0.

### 362 2.5.1 Sensor uncertainty

363 The overall accuracy-~~(i.e., integrated uncertainties)~~ of every SeaFET™ sensor was evaluated by  
364 quantifying all sources of potential uncertainty when calculating a final  $pH_t$  from the SeaFET™  
365 (Table 2). The  $pH_t$  uncertainty introduced by calibration method was calculated as the absolute  
366 difference between the “true  $pH_t$ ” and the final sensor  $pH_t$  derived from either factory calibration,  
367 the single-point *in situ* calibration, or multi-point *in situ* calibration. The “true  $pH_t$ ” was  
368 calculated using CO2SYS dissociation constants by Lueker et al., (2000) and Uppström, (1974)  
369 with measured  $TCO_2$  and TA via the VINDTA 3C,  $TCO_2$  and  $pCO_2$  measured by the BoL for  
370 discrete samples (e.g., SeaFET™<sub>268</sub>), and  $pCO_2$  and TA (TA-S equation, Evans et al. 2015) for  
371 continuous samples (SeaFET™<sub>397</sub>). A one-way analysis of variance (ANOVA) and the root  
372 mean square error (RMSE) were run and calculated in order to compare the  $pH_t$  values from both  
373 electrodes on SeaFET™<sub>397</sub> across calibration methods against the  $pH_t$  values from the BoL. The  
374 BoL at the APSH sampled every 5 min which produced 256 comparable sample points with a  
375 time alignment disparity that ranged from 0 – 120 s against SeaFET™<sub>397</sub>. The potential  $pH_t$   
376 uncertainty based on the thermistor was calculated by using the absolute difference between the  
377 thermistor derived temperature and that measured by the SBE 16plusV2 ( $T_{diff}$ ) from the OARC  
378 test tank deployments and the Kasitsna Bay SeaFETs™<sub>395, 396</sub> against the Seldovia data sonde 10  
379 km away. Finally, an average inter-sensor variability uncertainty term was calculated as the  
380 difference between the two SeaFETs™<sub>395, 396</sub> deployed side-by-side in Kasitsna Bay after a  
381 single-point *in situ* calibration was performed. All uncertainty terms were calculated and collated  
382 based on our evaluations from the Alaska deployed SeaFETs™<sub>395, 396, 397</sub>, while SeaFET™<sub>268</sub>  
383 deployed at Sentry Shoal was only included when determining the accuracy uncertainty term.  
384 Due to the disparity between reference samples for the Kasitsna Bay SeaFETs™<sub>395, 396</sub> and  
385 Sentry Shoal SeaFET™<sub>268</sub> (two discrete reference samples) to that at the ASPH SeaFET™<sub>397</sub>  
386 (256 reference samples), only the average calculated difference (SeaFET™  $pH_t$  – “true  $pH_t$ ”) for  
387 each calibration method and electrode was used from the APSH SeaFET™<sub>397</sub> and then collated  
388 with the other reference points from the Kasitsna Bay and Sentry Shoal SeaFETs™<sub>395, 396, 268</sub>.

389

Formatted: Font: Not Bold

## 390 2.5.2 $pH_t$ time series analysis

391  
392 Final time series analysis was examined in the time and frequency domain using the Mathworks  
393 software MATLAB (V. 2016a). Power spectral density was determined via Welch’s method  
394 using the pwelch function in MATLAB. Time series data was resampled and linearly  
395 interpolated in order to compensate for the missing data points that occurred when sensors  
396 arbitrarily stopped sampling.

397

## 398 3 Results

399

### 400 3.1 Test tank and field conditions

401

402 Finalized (i.e., calibrated)  $pH_t$  values from the first test tank deployment produced two different  
403 values, of which each was dependent on whether the calibration coefficient from the header file  
404 or the disc file was selected, the result was a difference of ~0.0011 units for both the internal and  
405 external electrodes. Because sensors were stored in tris buffer that lacked the addition of bromide  
406 between tank deployments and before field deployments, an environmental conditioning period  
407 was required for each of the Alaska SeaFETs™<sub>395, 396, 397</sub> once submerged in their respective



408 field sites. Thus, any determination of SeaFET<sup>TM</sup> pH<sub>t</sub> accuracy and conditioning period from  
409 tank deployments were inconclusive and will not be considered henceforth. No SeaFETs<sup>TM</sup><sub>395, 396,</sub>  
410 <sub>397, 268</sub> displayed signs of biofouling or low battery power upon recovery.

411  
412 SeaFET<sup>TM</sup><sub>397</sub> deployed in parallel with the BoL at the APSH experienced a tank failure  
413 on 8 April 2017 resulting in the sensor's emergence for 24 h. In addition, missing temperature  
414 and salinity values resulted in gaps of pH<sub>t</sub> measurements over the entire deployment. The BoL  
415 experienced flow control issues when initial deployment occurred on 6 March 2017 and was not  
416 online until 18 April 2017 but, then, operated nearly consistently until 24 May 2017. All pH<sub>t</sub> and  
417 temperature comparisons were, therefore, made beginning on 18 April 2017.

418  
419 Due to the *in situ* environmental conditioning period of the Kasitsna Bay SeaFETs<sup>TM</sup><sub>395,</sub>  
420 <sub>396,</sub> calibration was performed using the initial reference sample collected on 18 March 2017,  
421 03:00 UTC and again with the reference sample collected on 3 June 2017, 03:00 UTC. Due to  
422 high variance between duplicate reference samples (SD: 0.08 pH<sub>t</sub>) on 19 March 2017, 15:00  
423 UTC, this reference was discarded and not used for comparison or calibration. The Sentry Shoal  
424 SeaFET<sup>TM</sup><sub>268</sub> underwent one maintenance and cleaning procedure, including a battery change,  
425 during the ~5-month deployment (Table 1). One calibration sample (19 July 2016) and one  
426 reference sample (9 November 2016) were averaged from duplicate rather than triplicate  
427 replicates due to large variance from one of the replicate samples. The reference sample taken on  
428 23 August 2016, 17:00 UTC was discarded as temperature and salinity data were missing and  
429 SeaFET<sup>TM</sup><sub>268</sub> pH<sub>t</sub> could not be calculated. The final reference sample (UTC: 9 November 2016,  
430 17:05) was taken 5 min after SeaFET<sup>TM</sup><sub>268</sub> sampled on 9 November 2016, 17:00 UTC.

### 431 432 **3.2 Thermistor response: test tank deployment**

433  
434 The internal thermistor amongst the SeaFETs<sup>TM</sup><sub>395, 396, 397</sub> had a difference of less than 0.2 °C  
435 over the entirety of the second and third tank deployments. All thermistor derived temperature  
436 values had good alignment with the SBE 16plusV2 temperature, and consistently recorded a  
437 slightly higher temperature. The discrepancy between the thermistor temperature and  
438 SBE16plusV2 was minimal, and reached a maximum of 0.378 (logged by SeaFET<sup>TM</sup><sub>395</sub>) during  
439 any time over all tank deployments. The average discrepancy, however, was ~0.21 °C when  
440 averaging across all SeaFETs<sup>TM</sup><sub>395, 396, 397</sub> and all times—**resulting in a 0.003 pH uncertainty.** -

### 441 442 **3.3 Field performance**

443  
444 SeaFET<sup>TM</sup><sub>397</sub> deployed alongside the BoL appeared stable throughout its entire deployment and  
445 tracked the pH<sub>t</sub> derived from the BoL well (Fig. 2). Errant spikes were present from both  
446 electrodes throughout periods before 18 April 2017, which were a result of plumbing changes  
447 that occurred to the APSH incoming seawater. On 10 April 2017 the internal thermistor, BoL  
448 temp, and BoL salinity fluctuated by 3 °C and 14, respectively, over a 12 h period. These  
449 anomalies were removed from analysis. Salinity remained relatively stable throughout the rest of  
450 the deployment and ranged from 30.0 – 32.1. The pH<sub>t</sub> uncertainty (~~SeaFET<sup>TM</sup> “true” pH<sub>t</sub>~~)  
451 decreased, and the accuracy of the SeaFET's<sup>TM</sup><sub>397</sub> internal electrode improved once the *in situ*  
452 single-point and multi-point calibrations were performed with a RMSE decreasing from 0.5455  
453 pH<sub>t</sub> units under factory calibration, 0.0361 pH<sub>t</sub> units for *in situ* single-point calibration and

454 0.0273  $\text{pH}_t$  units for the *in situ* multi-point calibration. The external electrode also improved  
455 accuracy with *in situ* single-point and multi-point calibrations with an RMSE of 0.1077 under  
456 factory calibration, 0.0390 for *in situ* single-point calibration and 0.0388 for the *in situ* multi-  
457 point calibration (Fig. 2). There was a significant difference in the reduction of the  $\text{pH}_t$   
458 uncertainty for both the internal and external electrodes when utilizing *in situ* single-point and  
459 multi-point calibration coefficients compared to the factory calibration coefficients (Table 32). In  
460 addition, there was a significant decrease in the  $\text{pH}_t$  uncertainty when using the *in situ* multi-  
461 point calibration coefficients rather than the *in situ* single-point method for the internal electrode,  
462 but not for the external electrode (Table 32). The  $\text{pH}_t$  uncertainty of the internal electrode  
463 decreased from 0.0294 units with an *in situ* single-point calibration to 0.0224 units after an *in*  
464 *situ* multi-point calibration. It should be noted that the time alignment disparity which ranged  
465 from 0 – 120 s is not considered a significant source of discrepancy as only 4 sample points out  
466 of the 256 comparable points were  $> 0.03$  units (i.e., only 4 comparable points greater than the  
467 average  $\text{pH}_t$  uncertainty found after calibration) between any one 5 min sample taken by the  
468 BoL. The internal thermistor of SeaFET<sup>TM</sup><sub>397</sub> tracked the recorded BoL temperature trend fairly  
469 (Fig. 3), but had a greater magnitude discrepancy than its test tank deployment ( $\sim 0.21$  °C). On  
470 average, the thermistor temperature had an absolute difference of 2.83 °C (SD 0.35) from 18  
471 April 2017 – 6 June 2017, which would result in a  $\text{pH}_t$  uncertainty of  $\sim 0.044$  units. SeaFET<sup>TM</sup><sub>397</sub>  
472 was not fully submerged in the conical tank leaving the top portion susceptible to air temperature  
473 fluctuations which could have affected the thermistor readings.  
474

475 The SeaFETs<sup>TM</sup><sub>395, 396</sub> in Kasitsna Bay improved their accuracy after an *in situ* single-  
476 point calibration was performed (Fig. 4), however, this was only the case when sensors were not  
477 conditioned as calibration performed after the conditioning period reduced accuracy (Fig. 5)  
478 **when comparing against discrete reference samples**. It should be noted that only the  $\text{pH}_t$  recorded  
479 by both SeaFETs<sup>TM</sup><sub>395, 396</sub> at times of the reference samples had precise salinity and temperature  
480 (temperature and salinity recorded with reference sample rather than thermistor derived  
481 temperature) measurements as all other measurements were calculated from salinity measured by  
482 the data sonde 10 km away, and with temperature derived from the onboard thermistor. The  $\text{pH}_t$   
483 recorded by the external electrode at a fixed salinity displayed little to no variance relative to  $\text{pH}_t$   
484 calculated with data sonde salinity ( $< 0.02$   $\text{pH}_t$  difference: average whether conditioned or non-  
485 conditioned to environment). The average  $\text{pH}_t$  uncertainty from both SeaFETs<sup>TM</sup><sub>395, 396</sub> reduced  
486 by approximately half for the internal electrode when not conditioned to the environment after an  
487 *in situ* single-point calibration was performed (0.1072 and 0.1394 to 0.0475 and 0.0741 units,  
488 respectively), while the external electrode improved only minimally from 0.0988 and 0.0963 to  
489 0.0610 and 0.0894 units, respectively (Fig. 4). When *in situ* single-point calibration was  
490 performed after the SeaFETs<sup>TM</sup><sub>395, 396</sub> were conditioned (i.e., calibrated with reference sample  
491 taken on 4 June 2017, 03:00 UTC), the  $\text{pH}_t$  uncertainty for the internal electrode reduced only  
492 minimally from factory calibration: 0.1072 and 0.1394 to 0.0896 and 0.1240 units, respectively  
493 (Fig. 5a, b). Conversely, the  $\text{pH}_t$  error for the external electrode increased from 0.0988 and  
494 0.0963 to 0.1011 and 0.1480, respectively (Fig 5c, d).  
495

496 Both SeaFETs<sup>TM</sup><sub>395, 396</sub> displayed low inter-sensor variability for the internal electrode,  
497 and high for the external electrode after *in situ* single-point calibration was performed on sensors  
498 not conditioned to the environment (Fig. 6, gray circles). The mean anomaly between both  
499 SeaFET's<sup>TM</sup><sub>395, 396</sub> internal electrodes was 0.0525 units, whereas the external mean anomaly was

500 0.145 units. When measurements taken before the sensor was conditioned to the environment  
501 (blue shaded region Fig. 6) were removed from analysis, the mean anomaly changed by < 0.006  
502 units for both electrodes. Inter-sensor variability for both electrodes once conditioned, and after  
503 *in situ* single-point calibration, was < 0.05 units: 0.0409 and 0.0461 units for the internal and  
504 external electrodes, respectively (Fig. 6, black circles). When measurements recorded before the  
505 sensors were conditioned to the environment were removed (blue shaded region Fig. 10), the  
506 anomaly decreased further, < 0.015 units for both electrodes.

507  
508 Thermistor readings on both SeaFETs<sup>TM</sup><sub>395, 396</sub> tracked the temperature at the Seldovia  
509 site well, however errant spikes occurred around 18 April 2017 and again around 10 May 2017,  
510 and continued till the end of the deployment (Fig. 7). The absolute average difference between  
511 the thermistor values and the Seldovia data sonde was 0.281 °C (SD 0.295), nearly identical to  
512 the difference displayed during the test tank deployments, average 0.21 °C.

513  
514 At Sentry Shoal, temperature and salinity seasonally fluctuated and ranged from 8.71 –  
515 21.8 °C and 23.4 – 29.4, respectively. ~~Based on the overall accuracy of the internal and external  
516 electrodes, there was no clear distinction as to which provided the more robust measurement with  
517 greater accuracy between the internal and external electrodes~~ after *in situ* single-point calibration  
518 was performed. While the external electrode did display a lower pH<sub>t</sub> average uncertainty, this  
519 was based on only two reference points, one of which had a time discrepancy of 5 min (9  
520 November 2016, 17:05 UTC). Only two reference samples were comparable against  
521 SeaFET<sup>TM</sup><sub>268</sub> pH<sub>t</sub> due to the loss of salinity and temperature data on 23 August 2016, 17:00 UTC.  
522 Reference samples on 26 September 2016 and 9 November 2016 were, therefore, compared  
523 using the new calibration coefficients determined after redeployment on 27 August 2016. The  
524 average pH<sub>t</sub> uncertainty was < 0.0115 units for both electrodes (Fig. 8) compared to average pH<sub>t</sub>  
525 uncertainties of 0.0244 and 0.0560 units for the internal and external electrodes, respectively, if  
526 initial calibration coefficients from 19 July 2016 were retained. The low pH<sub>t</sub> uncertainty (<  
527 0.0137 units) determined after the *in situ* single-point calibration, however, was still greater than  
528 the average pH<sub>t</sub> uncertainty under factory calibration: < 0.005 units for both electrodes (Fig 8).

### 529 3.4 Spectral analysis

530  
531 All SeaFETs<sup>TM</sup><sub>395, 396, 397, 268</sub> displayed a mixed semi-diurnal tidal response during all field  
532 deployments (Fig. 9). SeaFETs<sup>TM</sup><sub>395, 396</sub> at Kasitsna Bay had a stronger amplitude response at a  
533 frequency of two cycles d<sup>-1</sup>, whereas SeaFET<sup>TM</sup><sub>397</sub> had a greater amplitude at one cycle d<sup>-1</sup> (Fig.  
534 9a, c, d). All three SeaFETs<sup>TM</sup><sub>395, 396, 397</sub> in Alaskan waters had a strong amplitude signal of 1  
535 cycle every 21 days, with an addition signal of one cycle every three days for SeaFET<sup>TM</sup><sub>397</sub>. The  
536 amplitude signal for SeaFET<sup>TM</sup><sub>397</sub> shifted depending on source of measurement (BoL, internal or  
537 external electrode), however, all measurement sources followed the same frequency pattern (Fig  
538 9a). SeaFET<sup>TM</sup><sub>268</sub> displayed a strong signal at a frequency of zero as well as at one and two  
539 cycles d<sup>-1</sup> (Fig 9a).

### 540 3.5 Intrinsic uncertainty and accuracy

541  
542 Among the calculated potential sources of uncertainty in pH<sub>t</sub>, inter-sensor variability (difference  
543 between SeaFET's<sup>TM</sup> pH<sub>t</sub>) and sensor accuracy produced the greatest uncertainty discrepancies

546 for the internal and external electrodes under factory calibration (Fig. 10). The  $pH_t$  uncertainty  
547 (i.e., overall sensor accuracy) for the internal electrode reduced a greater degree than the external  
548 electrode at every ordinal calibration method: factory, *in situ* single-point, to *in situ* multi-point  
549 calibration (Fig. 10). This was not the case for the external electrode, however, as the overall  $pH_t$   
550 accuracy was greater when factory calibration was used compared to an *in situ* single-point  
551 calibration was performed after the sensor was conditioned. The thermistor uncertainty (i.e.,  
552 uncertainty when calculating  $pH_t$  based on the thermistor temperature rather than a more accurate  
553 temperature gauge) produced a  $pH_t$  uncertainty of 0.0044 units, and was based on the recorded  
554 values by SeaFETs<sup>TM</sup><sub>395, 396</sub>. Even though the temperature-derived values from the thermistor of  
555 SeaFETs<sup>TM</sup><sub>395, 396</sub> were compared against a data sonde 10 km away, the average  $T_{diff}$  values were  
556 consistent with the  $T_{diff}$  calculated from the test tank deployments (within 0.07°C) and, therefore,  
557 provided an adequate resolution to determine a thermistor uncertainty value.

558  
559

#### 4 Discussion

560

561 Obtaining accurate and precise measurements of pH in nearshore coastal waters is crucial for  
562 understanding changing trends, dynamics, and current baselines of acidification in these—  
563 “susceptible to change”—marine domains. For dynamic nearshore systems, the current standard  
564 of OA weather (carbonate chemistry variability on timescales of days to months) accuracy  
565 should have an uncertainty no greater than 0.02 pH units according to the Global Ocean  
566 Acidification Observing Network (Newton et al. 2015). Previous evaluations of the SeaFET<sup>TM</sup>  
567 sensor package have demonstrated accuracy for both electrodes to be better than 0.02 pH units,  
568 with a range between 0.01 – 0.04 units for the internal electrode in more dynamic environments  
569 (Bresnahan et al., 2014; Gonski, 2018; Martz et al., 2010). Based on our findings, we observed  
570 an accuracy range of 0.009 – 0.148  $pH_t$  units after sensors were conditioned and *in situ* single-  
571 point or multi-point calibrations were performed for the internal and external electrodes. This  
572 range decreased when SeaFETs<sup>TM</sup><sub>395, 396</sub> from Kasitsna Bay were calibrated with reference  
573 samples taken at initial deployment (i.e., non-conditioned to environment). For SeaFET<sup>TM</sup><sub>397</sub>, the  
574 internal electrode’s accuracy was nearly identical to that of the external electrode after an *in situ*  
575 multi-point calibration (Fig. 2), suggesting that the internal electrode can produce a highly  
576 precise  $pH_t$  measurement comparable to the BoL with an accuracy meeting the standards of the  
577 OA weather measurements (Newton et al. 2015). This is not to suggest that the SeaFET<sup>TM</sup> can  
578 replace the BoL, particularly because the BoL can capture multiple carbonate chemistry  
579 measurements thereby fully constraining the system and identifying potential decoupling of the  
580 carbonate system in estuarine waters (Bandstra et al., 2006; Hales et al., 2016). Nonetheless, the  
581 SeaFET<sup>TM</sup> can provide an accurate measurement of  $pH_t$  in nearshore waters when SeaFET<sup>TM</sup>  
582 operation is executed with high precision.

583

584 SeaFETs<sup>TM</sup><sub>397, 268</sub> deployed at the APSH and at Sentry Shoal displayed the lowest  
585 uncertainty and greatest precision of  $pH_t$  measurements (Fig. 2 and 8). In both instances, the  
586 SeaFETs<sup>TM</sup><sub>397, 268</sub> were adequately conditioned (i.e., subjected to *in situ* conditions for ~50 days)  
587 before calibration was performed. The greater overall accuracy displayed by the SeaFET<sup>TM</sup><sub>268</sub> at  
588 Sentry Shoal may be due to the fact that the sensor was exposed to *in situ* conditions for a longer  
589 period of time and re-calibrated multiple times to the same environment. Further, calibration and  
590 reference sample  $pH_t$  was derived from  $TCO_2$  and  $pCO_2$  processed by the BoL at Sentry Shoal  
591 and from  $pCO_2$  (also measured by BoL) and the TA-salinity relationship (Evans et al. 2015) at

592 the APSH. It is unclear as to why the sensor accuracy of both Kasitsna Bay SeaFETs™<sup>395, 396</sup>  
593 was substantially less than the SeaFETs™<sup>397, 268</sup> at the APSH or Sentry Shoal. A potential reason  
594 for the low accuracy may be that sensors were calibrated at a reference point that was extreme  
595 relative to the time series pH<sub>t</sub> signal—that is, calibrated at a time of high variability. In this case,  
596 performing an *in situ* multiple-point calibration could have reduced the uncertainty and increased  
597 the accuracy. While previous studies have found that collection and preservation of calibration  
598 and reference samples can result in a decrease in accuracy depending on operator experience  
599 (McLaughlin et al., 2017), the operator in this study was considered to have substantial  
600 experience conducting such operations used in this evaluation. In addition, given the increased  
601 pH<sub>t</sub> variability over a short temporal period—which can be seen at the end of the Kasitsna Bay  
602 deployment (Fig. 4 and 5)—and the low discrepancy between duplicate reference samples, the  
603 former reasoning (i.e., calibrated to an extreme reference point) is a more reasonable explanation  
604 for the reduced accuracy by the Kasitsna Bay SeaFETs™<sup>395, 396</sup> than operator experience. We re-  
605 iterate here that reference sample temperature and salinity were used to calculate SeaFET™ pH<sub>t</sub>  
606 at the time points in which sensor pH<sub>t</sub> and reference sample pH<sub>t</sub> were compared, thus salinity  
607 was not a confounding factor.

608  
609 Despite the lower accuracy of the Kasitsna Bay SeaFETs™<sup>395, 396</sup>, the two sensors  
610 provided a better insight of inter-sensor variability for non-conditioned to the environment and  
611 conditioned electrodes. After *in situ* single-point calibration for conditioned sensors, the average  
612 inter-sensor variability decreased for the internal electrode by ~80%, and >300% for the external  
613 electrode (Fig. 6). The inter-sensor variability reported here was still greater than previous  
614 findings (Kapsenberg et al., 2017), however, the comparison made in this study was done in the  
615 field compared to controlled laboratory conditions as in Kapsenberg et al. (2017). And while  
616 non-homogenized water could lead to anomalies in pH<sub>t</sub> measurements by the Kasitsna Bay  
617 SeaFETs™<sup>395, 396</sup>, it is unlikely that water was consistently non-homogenized over the entirety of  
618 a deployment at a distance of < 20 cm (distance between electrodes on each SeaFET™).  
619 Furthermore, due to the dynamic nature of Kachemak Bay, where the tidal exchanges are  
620 extreme, averaging 4.73 m, it is unlikely that micro-heterogeneity of seawater is the driving force  
621 behind the observed differences in pH<sub>t</sub> measurements that were observed between SeaFETs™<sup>395,</sup>  
622 <sup>396</sup>. There was a tradeoff for a decrease in inter-sensor variability, as the *in situ* single-point  
623 calibration performed after sensors were conditioned resulted in a decrease in accuracy compared  
624 to an *in situ* single-point calibration performed for sensors not conditioned to the environment. It  
625 should be noted that we do not consider salinity to be a potential source of uncertainty for inter-  
626 sensor variability because the pH<sub>t</sub> difference using data sonde salinity compared to a fixed  
627 salinity resulted in an anomaly of < 0.005 units.

628  
629 The influence of rapid environmental variability should be acknowledged here as this can  
630 create uncertainty in autonomous sensor operation and accuracy (Tamburri et al. 2011).  
631 While the temperature changes due to rapid environmental change in Kasitsna Bay equate to a  
632 potential 0.011 discrepancy in pH, previous evaluation of these sensors show that rapid response  
633 to temperature changes should be negligible and result in uncertainties below the accuracy  
634 assured when applying an average temperature coefficient (k<sub>T</sub>), which can result in discrepancies  
635 of <0.015 pH units (Bresnahan et al. 2014). Rapid changes in salinity could also result in  
636 uncertainties regarding SeaFET™ accuracy and may be responsible for the noisier signal  
637 observed by the external electrode for the SeaFETs™<sup>395, 396</sup> deployed in Kasitsna Bay. The

Formatted: Indent: First line: 1.27 cm

Formatted: Font: (Default) Times New Roman, Not Bold

Formatted: Font: (Default) Times New Roman, Not Bold

Formatted: Font: (Default) Times New Roman, Not Bold

Formatted: Font: (Default) Times New Roman, Not Bold

Formatted: Font: (Default) Times New Roman, Not Bold

638 greatest salinity change within a 3 h period observed in Kasitsna Bay was 3.90. Given that the  
639 mean salinity at the deployment site was 31.8, a mismatch in timing here, or lag in response,  
640 could equate to pH changes as great as 0.053 units—although this likely a high estimate as this  
641 was the maximum difference within a 3 h period. It should be noted that rapid salinity changes  
642 would only affect the external electrode as the internal electrode is insensitive to changes in  
643 salinity. Due to the uncertainties that can emerge from rapid environmental variability, we  
644 reiterate the benefits of an operator understanding the deployment site as this will enhance data  
645 collection by the SeaFET™.

Formatted: Font: (Default) Times  
New Roman, Not Bold

646  
647 The Sentry Shoal SeaFET™<sub>268</sub> had the lowest average pH<sub>t</sub> uncertainty for both electrodes  
648 after *in situ* single-point calibration was performed, however, these were still greater than the pH<sub>t</sub>  
649 uncertainty determined using the factory calibration coefficients. This specific example  
650 highlights two possibilities: (1) the role of inter-sensor variability, as this may be a coincidental  
651 case given the uncertainty observed when quantifying inter-sensor variability, and (2) the  
652 influence of variance within a calibration sample set. For the case of SeaFET™<sub>268</sub>, the replicate  
653 calibration samples collected on 19 July 2016 and 2 September 2016 for the first and second  
654 deployments had standard deviations of 0.016 and 0.005 pH<sub>t</sub> units, respectively. ~~For instances of~~  
655 ~~generally~~~~When -close agreement between-~~factory and *in situ* calibrated data produce final pH<sub>t</sub>  
656 values in close agreement, it is important to recognize that the variance in the calibration sample  
657 set may contribute to better agreement between factory calibrated sensor pH<sub>t</sub> data and average  
658 discrete sample pH<sub>t</sub> measurements. It should also be noted that pre-deployment calibration can  
659 provide highly accurate measurements by the Honeywell Durafet (internal electrode), however,  
660 matching exact conditions to those at the field site are necessary (Johnson et al., 2017), and this  
661 was not likely the case for the factory provided calibration coefficients.

Formatted: Font: (Default) +Body  
(Calibri)

662  
663 The evaluation of SeaFET™ performance presented here corroborates and contrasts with  
664 previous studies examining the overall accuracy and precision of pH<sub>t</sub> measurements made by  
665 these oceanographic instruments. While the accuracy of two SeaFETs™<sub>397, 268</sub> fall well within  
666 the range determined from previous studies, the accuracy of SeaFETs™<sub>395, 396</sub> at Kasitsna Bay  
667 lay outside the bounds of what has been reported in the primary literature (Bresnahan et al.,  
668 2014; Gonski et al., 2018; Johnson et al., 2017; Kapsenberg et al., 2017; Martz et al., 2010). For  
669 example, Bresnahan et al. (2014) describes intrinsic Durafet uncertainties less than 0.03 units,  
670 but this varied depending on the validating reference source (e.g., spectrophotometric pH or pH<sup>est</sup>  
671 from O<sub>2</sub>). One reason as to why our the Kasitsna Bay SeaFET's™ uncertainties differed from  
672 Bresnahan et al. (2014) may be due to the fact that calibration was performed ~78 days after  
673 deployment. Thus, we suggest that in a highly dynamic area such as Kasitsna Bay, calibration  
674 should be performed immediately after conditioning. While there is no way to officially conclude  
675 that this could have reduced uncertainty, it is one potential source of discrepancy. Following  
676 current best practices in Bresnahan et al. (2014) may yield robust measurements, however, the  
677 utility of our assessment describes the importance of knowing when to take calibration samples  
678 as a means to decrease uncertainties. Nevertheless, it is relevant to report the potential  
679 uncertainties possible when operating SeaFETs™ as a multitude of factors can influence the  
680 overall accuracy (e.g., operator, sample preservation, electrode conditioning, calibration  
681 measurements), therefore, the potential uncertainties calculated in this study represent the upper  
682 limit of an average uncertainty compiled from four different SeaFETs™ (Fig. 10). The utility of  
683 such an analysis provides a confidence in SeaFET™ operation, and highlights all the potential



684 uncertainties that need to be considered when deploying the sensors in the field. For example, we  
685 have included a thermistor uncertainty term determined from the test tank and field deployments  
686 of the Alaska SeaFETs<sup>TM</sup><sub>395, 396, 397</sub>, even though a suitable solution around this issue would be to  
687 apply an offset to the thermistor temperature given it was compared to more robust temperature  
688 measurements conducted before field deployment. It should be noted, that in this case, the  
689 thermistor uncertainty observed from SeaFET<sup>TM</sup><sub>397</sub> against the BoL was excluded as the lag time  
690 between thermistor response and tank residence time likely confounded the comparison. The  
691 potential pH<sub>t</sub> uncertainties presented here should serve as a guide for SeaFET<sup>TM</sup> operators in  
692 order to better understand the source of an uncertainty and take the necessary steps to improve  
693 SeaFET<sup>TM</sup> measurements. Bresnahan et al. (2014) acknowledged that relying on the SeaFET<sup>TM</sup>  
694 for an accurate pH measurement should be viewed cautiously if additional biogeochemical  
695 sensors are not co-deployed to cross-validate the stability and accuracy of the SeaFET's<sup>TM</sup>  
696 electrodes, therefore, being fully aware of all the potential uncertainties presented here will only  
697 further aid SeaFET<sup>TM</sup> operators.

698  
699 The time series data provided by the SeaFET<sup>TM</sup> deployments in this study have expanded  
700 the scope-extent of recorded spatial-pH<sub>t</sub> variability along the North American west coast. The  
701 SeaFETs<sup>TM</sup><sub>395, 396</sub> deployed in Kasitsna Bay provide some of the first high temporal resolution  
702 measurements of pH<sub>t</sub> in this region. During this spring deployment, it appears that semi-diurnal  
703 tidal fluctuations are the dominant contributor to pH<sub>t</sub> variability with an additional cycle  
704 occurring every 21 days coinciding with the seasonal spring and neap tides (Fig. 9). The  
705 SeaFET<sup>TM</sup><sub>268</sub> at Sentry Shoal also displays a strong pH<sub>t</sub> response to the semi-diurnal mixed tidal  
706 cycle. A strong signal is also present at a frequency of zero, and is likely a result of the long,  
707 across-season, time series. That is, over the course of the entire deployment which went from  
708 summer into late fall, seasonal drivers of pH<sub>t</sub> (e.g., decrease in water temperature) confounded  
709 repetitive frequency patterns. In addition, Sentry Shoal may have a weaker tidal signature  
710 relative to other pH<sub>t</sub> modulators that do not follow a cyclical pattern such as water mass  
711 intrusion, inconsistent metabolic cycles from the end of summer into the fall season, and a shift  
712 to the rainy season.

713  
714 As an elaboration on the power spectral density analysis, we suggest this form of  
715 frequency analysis can be utilized to better understand the system in which a SeaFET<sup>TM</sup> is  
716 deployed, thus informing the operator as to what the drivers of their system are, and when to  
717 calibrate the sensor. It is possible that in a highly dynamic setting, the sensor could re-condition  
718 over time periods not resolved in a multi-point calibration sampling scheme, and this could  
719 enhance sensor inaccuracies. For example, in Kasitsna Bay, a strong semi-diurnal tide cycle was  
720 present, so upon redeployment in this area, if possible, the best calibration approach would be an  
721 *in situ* multi-point calibration between the Mixed semi-diurnal tidal cycle. Alternatively, if the  
722 system is not driven by a strong tidal signature (e.g., non-coastal region), an *in situ* single-point  
723 calibration may be a reasonable approach. It should be noted that while spectral analysis can be  
724 used as an additional tool to better calibrate the SeaFET<sup>TM</sup>, specific coastal environments with  
725 dynamic storm frequencies or varying photosynthesis and respiration cycles could obscure a  
726 clear driving frequency of pH change. In these situations, capturing the dynamic range (i.e.,  
727 multiple calibration samples over this period) of one of these events may be sufficient to provide  
728 best approach for robust calibration.

729

730 **5 Conclusion**

731  
732 The following evaluation of the Sea-Bird SeaFET™ helped elucidate the overall  
733 accuracy and highlighted the potential uncertainties and pitfalls of operating and obtaining pH<sub>t</sub>  
734 measurements by the internal and external electrode pair. We found that the internal electrode  
735 provided the more robust measurement in nearshore estuarine waters when an *in situ* multi-point  
736 calibration was performed (Fig. 10). The quantified potential pH<sub>t</sub> uncertainty is based  
737 specifically on our findings, whereas further results may minimize this uncertainty given  
738 additional evaluations. However, the results here provide an upper limit of the pH<sub>t</sub> uncertainty  
739 that may be observed when operating a Sea-Bird SeaFET™. Further, high temporal resolution  
740 pH<sub>t</sub> measurements in nearshore Canadian and Alaskan waters provide a better understanding of  
741 the drivers modulating pH on short timescales. Given the application, the Sea-Bird SeaFET™  
742 can provide a reliable and accurate pH<sub>t</sub> measurement which can be utilized to broaden the  
743 coverage of understanding pH variability in nearshore and open-ocean waters.  
744

745 **Acknowledgments**

746 The authors would like to thank Jeff Hetrick and Jacqueline Ramsey at the Alutiiq Pride  
747 Shellfish Hatchery for providing their facilities and services for this evaluation. We would also  
748 like to thank Angela Doroff at the Kasitsna Bay laboratory for providing facilities for SeaFET™  
749 deployments. Funding for this project was provided in part by the University of Alaska  
750 Fairbanks College of Fisheries and Ocean Sciences. WE and KP thank the Pacific Salmon  
751 Foundation and Environment Canada for providing the platform for deploying SeaFET 268, the  
752 University of Alaska Fairbanks Ocean Acidification Research Center for the long-term use of  
753 SeaFET 268, and the Tula Foundation for supporting their efforts with this work.  
754  
755

756 **References**

- 757 Bandstra, L., Hales, B. and Takahashi, T.: High-frequency measurements of total CO<sub>2</sub>: Method  
758 development and first oceanographic observations, *Mar. Chem.*, 100(1–2), 24–38,  
759 doi:10.1016/j.marchem.2005.10.009, 2006.
- 760 Barton, A., Hales, B., Waldbusser, G. G., Langdon, C. and Feely, R. A.: The Pacific oyster,  
761 *Crassostrea gigas*, shows negative correlation to naturally elevated carbon dioxide levels:  
762 Implications for near-term ocean acidification effects, *Limnol. Oceanogr.*, 57(3), 698–710,  
763 doi:10.4319/lo.2012.57.3.0698, 2012.
- 764 Bresnahan, P. J., Martz, T. R., Takeshita, Y., Johnson, K. S. and LaShomb, M.: Best practices for  
765 autonomous measurement of seawater pH with the Honeywell Durafet, *Methods Oceanogr.*, 9,  
766 44–60, doi:10.1016/j.mio.2014.08.003, 2014.
- 767 Caldeira, K. and Wickett, M. E.: Anthropogenic carbon and ocean pH, *Nature*, 425(6956), 365–  
768 365, doi:10.1038/425365a, 2003.
- 769 Chan, F., Barth, J. A., Blanchette, C. A., Byrne, R. H., Chavez, F., Cheriton, O., Feely, R. A.,  
770 Friederich, G., Gaylord, B., Gouhier, T., Hacker, S., Hill, T., Hofmann, G., McManus, M. A.,  
771 Menge, B. A., Nielsen, K. J., Russell, A., Sanford, E., Sevadjan, J. and Washburn, L.: Persistent



772 spatial structuring of coastal ocean acidification in the California Current System, *Sci. Rep.*, 7(1),  
773 2526, doi:10.1038/s41598-017-02777-y, 2017.

774 Dickson, A. G., Sabine, C. L. and Christian, J. R.: Guide to Best Practices for Ocean CO<sub>2</sub>  
775 Measurements., Report, North Pacific Marine Science Organization. [online] Available from:  
776 <http://www.oceandatapractices.net:80/handle/11329/249>, 2007.

777 Duarte, C. M., Hendriks, I. E., Moore, T. S., Olsen, Y. S., Steckbauer, A., Ramajo, L.,  
778 Carstensen, J., Trotter, J. A. and McCulloch, M.: Is Ocean Acidification an Open-Ocean  
779 Syndrome? Understanding Anthropogenic Impacts on Seawater pH, *Estuaries Coasts*, 36(2),  
780 221–236, doi:10.1007/s12237-013-9594-3, 2013.

781 Ekstrom, J. A., Suatoni, L., Cooley, S. R., Pendleton, L. H., Waldbusser, G. G., Cinner, J. E.,  
782 Ritter, J., Langdon, C., van Hooijdonk, R., Gledhill, D., Wellman, K., Beck, M. W., Brander, L.  
783 M., Rittschof, D., Doherty, C., Edwards, P. E. T. and Portela, R.: Vulnerability and adaptation of  
784 US shellfisheries to ocean acidification, *Nat. Clim. Change*, 5(3), 207–214,  
785 doi:10.1038/NCLIMATE2508, 2015.

786 Evans, W., Mathis, J. T. and Cross, J. N.: Calcium carbonate corrosivity in an Alaskan inland  
787 sea, *Biogeosciences*, 11(2), 365–379, doi:10.5194/bg-11-365-2014, 2014.

788 Evans, W., Mathis, J. T., Ramsay, J. and Hetrick, J.: On the Frontline: Tracking Ocean  
789 Acidification in an Alaskan Shellfish Hatchery, *PLOS ONE*, 10(7), e0130384,  
790 doi:10.1371/journal.pone.0130384, 2015.

791 Feely, R. A., Alin, S. R., Newton, J., Sabine, C. L., Warner, M., Devol, A., Krembs, C. and  
792 Maloy, C.: The combined effects of ocean acidification, mixing, and respiration on pH and  
793 carbonate saturation in an urbanized estuary, *Estuar. Coast. Shelf Sci.*, 88(4), 442–449,  
794 doi:10.1016/j.ecss.2010.05.004, 2010.

795 Feely, R. A., Alin, S. R., Carter, B., Bednaršek, N., Hales, B., Chan, F., Hill, T. M., Gaylord, B.,  
796 Sanford, E., Byrne, R. H., Sabine, C. L., Greeley, D. and Juranek, L.: Chemical and biological  
797 impacts of ocean acidification along the west coast of North America, *Estuar. Coast. Shelf Sci.*,  
798 183, Part A, 260–270, doi:10.1016/j.ecss.2016.08.043, 2016.

799 Gonski, S. F., Cai, W.-J., Ullman, W. J., Joesoef, A., Main, C. R., Pettay, D. T. and Martz, T. R.:  
800 Assessment of the suitability of Durafet-based sensors for pH measurement in dynamic estuarine  
801 environments, *Estuar. Coast. Shelf Sci.*, 200(Supplement C), 152–168,  
802 doi:10.1016/j.ecss.2017.10.020, 2018.

803 Hales, B., Suhrbier, A., Waldbusser, G. G., Feely, R. A. and Newton, J. A.: The Carbonate  
804 Chemistry of the “Fattening Line,” Willapa Bay, 2011–2014, *Estuaries Coasts*, 1–14,  
805 doi:10.1007/s12237-016-0136-7, 2016.

806 Harris, K. E., DeGrandpre, M. D. and Hales, B.: Aragonite saturation state dynamics in a coastal  
807 upwelling zone, *Geophys. Res. Lett.*, 40(11), 2720–2725, doi:10.1002/grl.50460, 2013.

808 Hofmann, G. E., Smith, J. E., Johnson, K. S., Send, U., Levin, L. A., Micheli, F., Paytan, A.,  
809 Price, N. N., Peterson, B., Takeshita, Y., Matson, P. G., Crook, E. D., Kroeker, K. J., Gambi, M.  
810 C., Rivest, E. B., Frieder, C. A., Yu, P. C. and Martz, T. R.: High-Frequency Dynamics of Ocean  
811 pH: A Multi-Ecosystem Comparison, *Plos One*, 6(12), e28983,  
812 doi:10.1371/journal.pone.0028983, 2011.

813 Johnson, K. S., Plant, J. N., Coletti, L. J., Jannasch, H. W., Sakamoto, C. M., Riser, S. C., Swift,  
814 D. D., Williams, N. L., Boss, E., Haentjens, N., Talley, L. D. and Sarmiento, J. L.:  
815 Biogeochemical sensor performance in the SOCCOM profiling float array, *J. Geophys. Res.-*  
816 *Oceans*, 122(8), 6416–6436, doi:10.1002/2017JC012838, 2017.

817 Kapsenberg, L., Bockmon, E. E., Bresnahan, P. J., Kroeker, K. J., Gattuso, J.-P. and Martz, T.  
818 R.: Advancing Ocean Acidification Biology Using Durafet® pH Electrodes, *Front. Mar. Sci.*, 4,  
819 doi:10.3389/fmars.2017.00321, 2017.

820 Kapsenberg, L. and Hofmann, G. E.: Ocean pH time-series and drivers of variability along the  
821 northern Channel Islands, California, USA, *Limnol. Oceanogr.*, 61(3), 953–968,  
822 doi:10.1002/lno.10264, 2016.

823 Kapsenberg, L., Kelley, A. L., Shaw, E. C., Martz, T. R. and Hofmann, G. E.: Near-shore  
824 Antarctic pH variability has implications for the design of ocean acidification experiments, *Sci.*  
825 *Rep.*, 5, srep09638, doi:10.1038/srep09638, 2015.

826 Khoo, K. H., Ramette, R. W., Culberson, C. H. and Bates, R. G.: Determination of hydrogen ion  
827 concentrations in seawater from 5 to 40.degree.C: standard potentials at salinities from 20 to  
828 45%, *Anal. Chem.*, 49(1), 29–34, doi:10.1021/ac50009a016, 1977.

829 Lueker, T. J., Dickson, A. G. and Keeling, C. D.: Ocean pCO<sub>2</sub> calculated from dissolved  
830 inorganic carbon, alkalinity, and equations for K-1 and K-2: validation based on laboratory  
831 measurements of CO<sub>2</sub> in gas and seawater at equilibrium, *Mar. Chem.*, 70(1–3), 105–119,  
832 doi:10.1016/S0304-4203(00)00022-0, 2000.

833 Martz, T., Send, U., Ohman, M. D., Takeshita, Y., Bresnahan, P., Kim, H.-J. and Nam, S.:  
834 Dynamic variability of biogeochemical ratios in the Southern California Current System,  
835 *Geophys. Res. Lett.*, 41(7), 2496–2501, doi:10.1002/2014GL059332, 2014.

836 Martz, T. R., Connery, J. G. and Johnson, K. S.: Testing the Honeywell Durafet® for seawater  
837 pH applications, *Limnol. Oceanogr. Methods*, 8(5), 172–184, doi:10.4319/lom.2010.8.172, 2010.

838 Martz, T. R., Daly, K. L., Byrne, R. H., Stillman, J. H. and Turk, D.: Technology for ocean  
839 acidification research: needs and availability, *Oceanography*, 28(2), 40–47, 2015.

840 Mathis, J. T., Cross, J. N. and Bates, N. R.: Coupling primary production and terrestrial runoff to  
841 ocean acidification and carbonate mineral suppression in the eastern Bering Sea, *J. Geophys.*  
842 *Res. Oceans*, 116(C2), C02030, doi:10.1029/2010JC006453, 2011a.

843 Mathis, J. T., Cross, J. N. and Bates, N. R.: The role of ocean acidification in systemic carbonate  
844 mineral suppression in the Bering Sea, *Geophys. Res. Lett.*, 38(19), L19602,  
845 doi:10.1029/2011GL048884, 2011b.

846 Mathis, J. T., Pickart, R. S., Byrne, R. H., McNeil, C. L., Moore, G. W. K., Juranek, L. W., Liu,  
847 X., Ma, J., Easley, R. A., Elliot, M. M., Cross, J. N., Reisdorph, S. C., Bahr, F., Morison, J.,  
848 Lichendorf, T. and Feely, R. A.: Storm-induced upwelling of high pCO<sub>2</sub> waters onto the  
849 continental shelf of the western Arctic Ocean and implications for carbonate mineral saturation  
850 states, *Geophys. Res. Lett.*, 39(7), L07606, doi:10.1029/2012GL051574, 2012.

851 Mathis, J. T., Cross, J. N., Monacci, N., Feely, R. A. and Stabeno, P.: Evidence of prolonged  
852 aragonite undersaturations in the bottom waters of the southern Bering Sea shelf from  
853 autonomous sensors, *Deep-Sea Res. Part II-Top. Stud. Oceanogr.*, 109, 125–133,  
854 doi:10.1016/j.dsr2.2013.07.019, 2014.

855 Mathis, J. T., Cross, J. N., Evans, W. and Doney, S. C.: Ocean Acidification in the Surface  
856 Waters of the Pacific-Arctic Boundary Regions, *Oceanography*, 28(2), 122–135,  
857 doi:10.5670/oceanog.2015.36, 2015a.

858 Mathis, J. T., Cooley, S. R., Lucey, N., Colt, S., Ekstrom, J., Hurst, T., Hauri, C., Evans, W.,  
859 Cross, J. N. and Feely, R. A.: Ocean acidification risk assessment for Alaska’s fishery sector,  
860 *Prog. Oceanogr.*, 136, 71–91, doi:10.1016/j.pocean.2014.07.001, 2015b.

861 Matson, P. G., Martz, T. R. and Hofmann, G. E.: High-frequency observations of pH under  
862 Antarctic sea ice in the southern Ross Sea, *Antarct. Sci.*, 23(6), 607–613,  
863 doi:10.1017/S0954102011000551, 2011.

864 McLaughlin, K., Dickson, A., Weisberg, S. B., Coale, K., Elrod, V., Hunter, C., Johnson, K. S.,  
865 Kram, S., Kudela, R., Martz, T., Negrey, K., Passow, U., Shaughnessy, F., Smith, J. E., Tadesse,  
866 D., Washburn, L. and Weis, K. R.: An evaluation of ISFET sensors for coastal pH monitoring  
867 applications, *Reg. Stud. Mar. Sci.*, 12, 11–18, doi:10.1016/j.rsma.2017.02.008, 2017.

868 Newton J.A., Feely R. A., Jewett E. B., Williamson P. & Mathis J.  
869 2015. Global Ocean Acidification Observing Network: Requirements and Governance Plan.  
870 Second Edition, GOA-ON, [http://www.goa-on.org/docs/GOA-ON\\_plan\\_print.pdf](http://www.goa-on.org/docs/GOA-ON_plan_print.pdf).  
871

872 Newton, J., Devol, A., Alford, M., Mickett, J., Sabine, C. and Sutton, A.: Nanoos Contributions  
873 to Understanding Ocean Acidification, *J. Shellfish Res.*, 31(1), 327–327, 2012.

874 Orr, J. C., Fabry, V. J., Aumont, O., Bopp, L., Doney, S. C., Feely, R. A., Gnanadesikan, A.,  
875 Gruber, N., Ishida, A., Joos, F., Key, R. M., Lindsay, K., Maier-Reimer, E., Matear, R., Monfray,  
876 P., Mouchet, A., Najjar, R. G., Plattner, G. K., Rodgers, K. B., Sabine, C. L., Sarmiento, J. L.,  
877 Schlitzer, R., Slater, R. D., Totterdell, I. J., Weirig, M. F., Yamanaka, Y. and Yool, A.:  
878 Anthropogenic ocean acidification over the twenty-first century and its impact on calcifying  
879 organisms, *Nature*, 437(7059), 681–686, doi:10.1038/nature04095, 2005.

880 Orr, J. C., J.-M. Epitalon, A. G. Dickson, and J.-P. Gattuso: Routine uncertainty propagation for  
881 the marine carbon dioxide system, *Marine Chemistry*, *in prep.*

882  
883 Riebesell, U. and Gattuso, J.-P.: Lessons learned from ocean acidification research, *Nat. Clim.*  
884 *Change*, 5(1), 12–14, doi:10.1038/nclimate2456, 2015.

885 Rudd, M. A.: What a Decade (2006–15) Of Journal Abstracts Can Tell Us about Trends in  
886 Ocean and Coastal Sustainability Challenges and Solutions, *Front. Mar. Sci.*, 4,  
887 doi:10.3389/fmars.2017.00170, 2017.

888 Steinhart, J. S. and Hart, S. R.: Calibration curves for thermistors, *Deep Sea Res. Oceanogr.*  
889 *Abstr.*, 15(4), 497–503, doi:10.1016/0011-7471(68)90057-0, 1968.

890 Sunda, W. G. and Cai, W.-J.: Eutrophication Induced CO<sub>2</sub>-Acidification of Subsurface Coastal  
891 Waters: Interactive Effects of Temperature, Salinity, and Atmospheric P-CO<sub>2</sub>, *Environ. Sci.*  
892 *Technol.*, 46(19), 10651–10659, doi:10.1021/es300626f, 2012.

893 Takeshita, Y., Martz, T. R., Johnson, K. S. and Dickson, A. G.: Characterization of an Ion  
894 Sensitive Field Effect Transistor and Chloride Ion Selective Electrodes for pH Measurements in  
895 Seawater, *Anal. Chem.*, 86(22), 11189–11195, doi:10.1021/ac502631z, 2014.

896 Tamburri, M. N., Johengen, T. H., Atkinson, M. J., Schar, D. W. H., Robertson, C. Y., Purcell,  
897 H., Smith, G. J., Pinchuk, A. and Buckley, E. N.: Alliance for Coastal Technologies, *Marine*  
898 *Technology Society Journal*, 45(1), 43–51, doi: 10.4031/MTSJ.45.1.4, 2011.

899 Uppström, L. R.: The boron/chlorinity ratio of deep-sea water from the Pacific Ocean, *Deep Sea*  
900 *Res. Oceanogr. Abstr.*, 21, 161–162, doi:10.1016/0011-7471(74)90074-6, 1974.

901 Waldbusser, G. G. and Salisbury, J. E.: Ocean Acidification in the Coastal Zone from an  
902 Organism's Perspective: Multiple System Parameters, Frequency Domains, and Habitats,  
903 *Annu. Rev. Mar. Sci.*, 6(1), 221–247, doi:10.1146/annurev-marine-121211-172238, 2014.

904 Yu, P. C., Matson, P. G., Martz, T. R. and Hofmann, G. E.: The ocean acidification seascape and  
905 its relationship to the performance of calcifying marine invertebrates: Laboratory experiments on  
906 the development of urchin larvae framed by environmentally-relevant pCO<sub>2</sub>/pH, *J. Exp. Mar.*  
907 *Biol. Ecol.*, 400(1–2), 288–295, doi:10.1016/j.jembe.2011.02.016, 2011.

908  
909  
910  
911  
912  
913  
914  
915  
916  
917  
918  
919

Formatted: Font: (Default) Times New Roman

Formatted: Normal, Indent: Left: -0.63 cm, Space Before: Auto, After: Auto, Outline numbered + Level: 1 + Numbering Style: Bullet + Aligned at: 0.63 cm + Tab after: 1.27 cm + Indent at: 1.27 cm, Pattern: Clear (White)

Formatted: Font: (Default) Times New Roman

Formatted: Font: (Default) Times New Roman, 12 pt

Formatted: Font: (Default) Times New Roman

Formatted: Font color: Custom Color(119,119,119)

920  
921  
922  
923  
924  
925  
926  
927

**Table 1.** Deployment regime of all four SeaFETs™ including deployment location, date, and calibration methods performed. \*Non-controlled source water pumped directly from Resurrection Bay, AK, USA.

Location (Tank or Field)	Date	SeaFET™ ID	Average reads frame <sup>1</sup>	Frames Burst <sup>1</sup>	Sampling Freq. (min)	Calibration method
APSH — <i>Tank</i>	5 – 8 October 2016	395, 396, 397	1	10	5	Factory
OARC — <i>Tank</i>	26 October – 3 November 2016	395, 396, 397	3	—	Continuous	Factory
OARC — <i>Tank</i>	26 January – 1 February 2017	395, 396, 397	1	10	180	Factory
APSH <i>Field*</i>	5 March – 6 June 2017	397	10	30	180	Factory, SP and MP <i>in situ</i>
Kachemak Bay <i>Field</i>	18 March – 4 June 2017	395, 396	10	30	180	Factory, SP <i>in situ</i>
Sentry Shoal <i>Field</i>	6 July – 23 August, 27 August – 28 November 2016	268	10	30	30	Factory, SP <i>in situ</i>

928  
929  
930  
931  
932  
933  
934  
935  
936  
937  
938  
939  
940  
941  
942  
943  
944  
945  
946  
947  
948  
949  
950

Factory: factory calibration; SP: *in situ* single-point calibration; MP: *in situ* multi-point calibration.

951  
952  
953  
954  
955  
956

**Table 2. Terms and definitions used to describe the evaluation of the Sea-Bird SeaFET™ based on observations specific to this study.**

Formatted: Font: Not Bold

Formatted: Font: Not Bold

Terms	Definiiton
<b>Uncertainty</b>	One or multiple factors that result in a discrepancy between SeaFET™ pH - "True pH" that are non-correctable
Accuracy Overall Accuracy	Difference between SeaFET™ pH - "True pH" Integrated uncertainties
"True pH <sub>t</sub> "	pH on the total scale measured by robust bench top methods: either VINDTA 3C or the Burke-o-lator
Variability	Specific difference in pH <sub>t</sub> between the internal or external electrodes on SeaFETs™ 395 and 396
<b>Mean Anomaly</b>	Average difference between the internal and external electrode pH <sub>t</sub>

957  
958  
959  
960  
961  
962  
963  
964  
965  
966  
967  
968  
969  
970  
971  
972  
973  
974  
975  
976  
977  
978  
979  
980

981  
 982  
 983  
 984  
 985  
 986  
 987  
 988

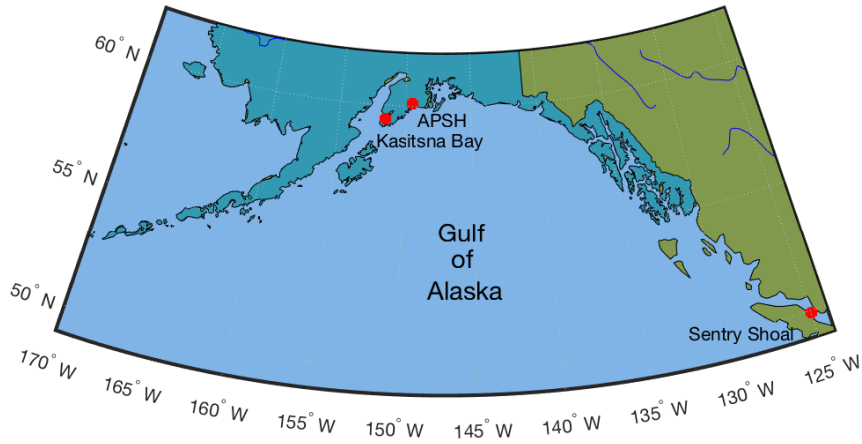
**Table 32.** One-way Analysis of variance comparing the pH<sub>t</sub> error (SeaFET<sup>TM</sup> pH<sub>t</sub> – BoL pH<sub>t</sub>) across calibration methods for both the internal and external electrodes onboard SeaFETs<sup>TM</sup><sub>268</sub> at Sentry Shoal (factory calibration and *in situ* single-point calibration) and SeaFET<sup>TM</sup><sub>397</sub> at the Alutiiq Pride Shellfish Hatchery (factory calibration, *in situ* single-point calibration, and *in situ* multi-point calibration). Bold type denotes statistical significance.

Site	Electrode	Source	SS	df	MS	F	p-value
APSH	Internal	Fac Cal. Vs. Single-point	27.5	1	27.5	4.96E+04	<b>&lt; 0.001</b>
		Error	0.225	406	0.001		
		Total	27.7	407			
APSH	External	Fac Cal. Vs. Single-point	0.681	1	0.681	536	<b>&lt; 0.001</b>
		Error	0.516	406	0.001		
		Total	1.19	407			
APSH	Internal	Factory Cal. vs. Multi-point	28.3	1	28.3	6.19E+04	<b>&lt; 0.001</b>
		Error	0.185	406	0.001		
		Total	28.5	407			
APSH	External	Factory Cal. vs. Multi-point	0.692	1	0.692	539	<b>&lt; 0.001</b>
		Error	0.521	406	0.001		
		Total	1.21	407			
APSH	Internal	Single-point vs. Multi-point	0.005	1	0.005	15.0	<b>&lt; 0.001</b>
		Error	0.143	406	0.000		
		Total	0.148	407			
APSH	External	Single-point vs. Multi-point	0.000	1	0.000	0.040	0.843
		Error	0.415	406	0.001		
		Total	0.415	407			

989  
 990  
 991  
 992  
 993  
 994  
 995  
 996  
 997  
 998  
 999  
 1000  
 1001  
 1002  
 1003  
 1004  
 1005  
 1006  
 1007  
 1008  
 1009  
 1010

1011  
1012  
1013  
1014  
1015

**Figure 1.**



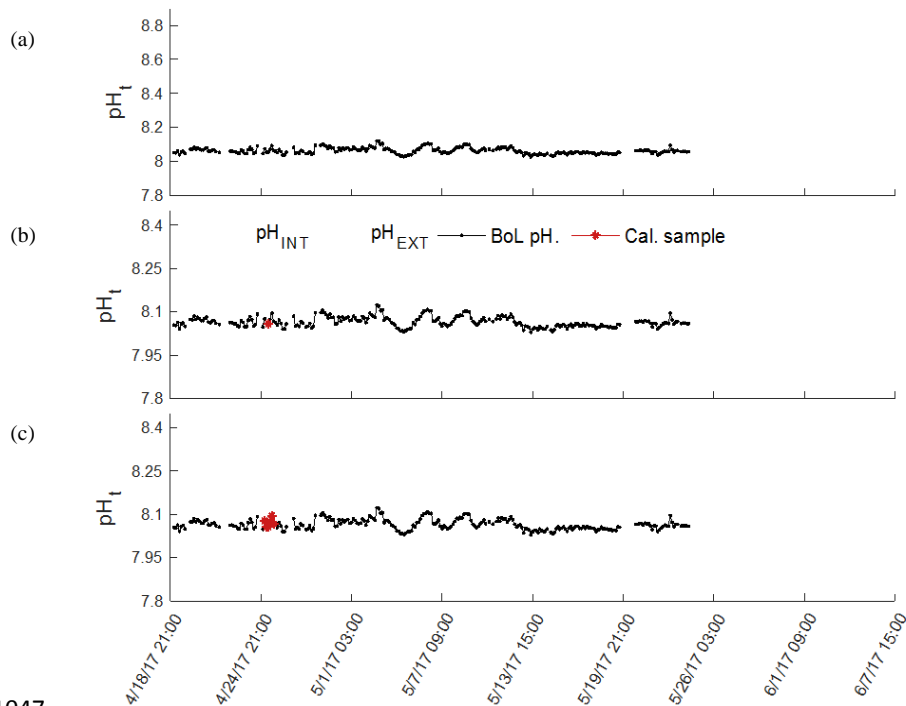
1016  
1017  
1018  
1019  
1020  
1021  
1022  
1023  
1024  
1025  
1026  
1027  
1028  
1029  
1030  
1031  
1032  
1033  
1034  
1035  
1036  
1037  
1038  
1039  
1040  
1041  
1042

Geographical map with locations of SeaFET™ field deployments along Alaska's, USA, south-central coast and one location in the Strait of Georgia, British Columbia, Canada.



1043  
1044  
1045  
1046

Figure 2.

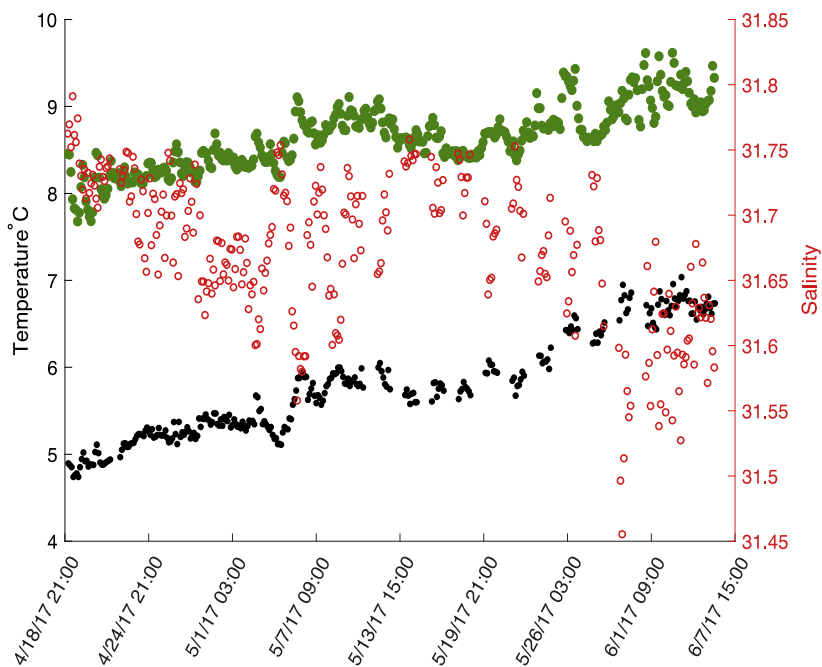


1047  
1048  
1049  
1050  
1051  
1052  
1053  
1054  
1055  
1056  
1057  
1058  
1059  
1060  
1061  
1062  
1063  
1064  
1065  
1066

pH<sub>t</sub> recorded by the internal (solid) and external (dashed) electrodes on SeaFET™<sub>397</sub> deployed in parallel with the BoL at the Alutiiq Pride Shellfish Hatchery. pH<sub>t</sub> from both electrodes is shown when derived using factory calibration (FC) coefficients (panel a), *in situ* single-point (SC) calibration coefficients (panel b), and *in situ* multi-point (MC) calibration coefficients (panel c). Black solid line is pH<sub>t</sub> derived from continuous pCO<sub>2</sub> measurements recorded by the BoL and derived TA from the TA-S relationship (Evans et al. 2015). Red circles are the calibration points from the BoL data.

1067  
1068  
1069  
1070

Figure 3.



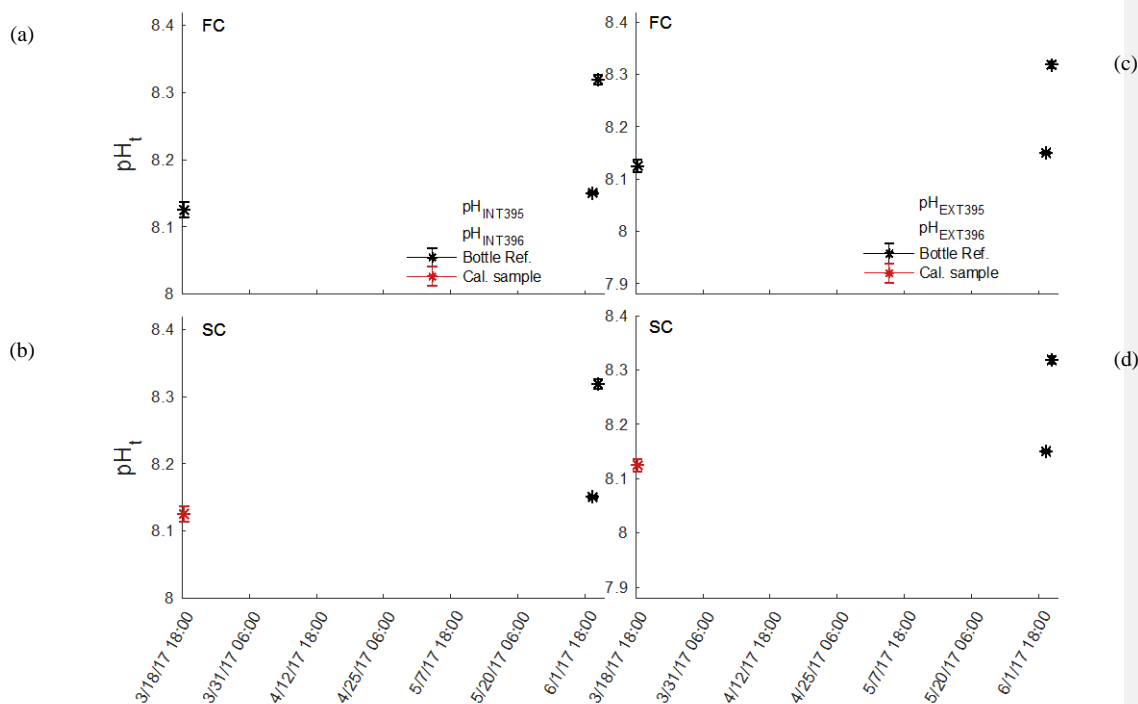
1071  
1072  
1073  
1074  
1075  
1076  
1077  
1078  
1079  
1080  
1081  
1082  
1083  
1084  
1085  
1086  
1087  
1088  
1089  
1090

Temperature derived from the internal thermistor on SeaFET<sup>TM</sup><sub>397</sub> (green circles) and the temperature recorded by the BoL (black circles) at the Alutiiq Pride Shellfish Hatchery from late winter through spring 2017. Salinity (red circles) recorded by the BoL on the right y-axis.

SeaFET<sup>TM</sup><sub>397</sub> was only partially submerged resulting in the top half of the sensor exposed to air temperature fluctuations.

1091  
 1092  
 1093  
 1094  
 1095  
 1096

Figure 4.

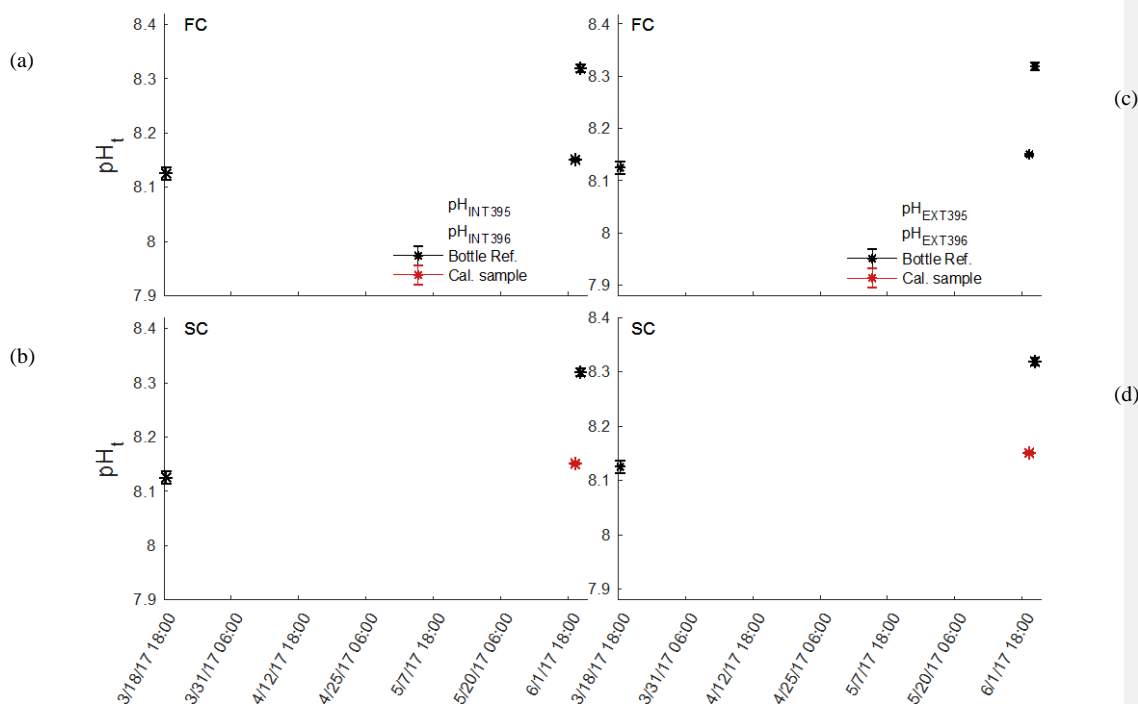


1097  
 1098  
 1099  
 1100  
 1101  
 1102  
 1103  
 1104  
 1105  
 1106  
 1107  
 1108  
 1109  
 1110  
 1111  
 1112  
 1113

Comparison of pH<sub>t</sub> recorded by the internal (panel a and b) and external (panel c and d) electrodes on SeaFET<sup>TM</sup><sub>395</sub> (blue) and SeaFET<sup>TM</sup><sub>396</sub> (purple) before they were conditioned to the environment (non-conditioned) deployed in Kasitsna Bay, AK, based on calibration method: factory calibration (FC) and *in situ* single-point (SC) calibration. Discrete reference samples (black asterisks) and calibration sample (red asterisks) were collected 36 and 12 h pre-SeaFET<sup>TM</sup> recovery, and < 24 h post-deployment, respectively. Temperature and salinity measurements collected on reference and calibration samples were used to derive SeaFET<sup>TM</sup> pH<sub>t</sub> at those given time points. All other SeaFET<sup>TM</sup> pH<sub>t</sub> measurements use thermistor temperature and salinity logged by Kasitsna Bay data sonde.

1114  
1115  
1116  
1117  
1118  
1119

Figure 5.

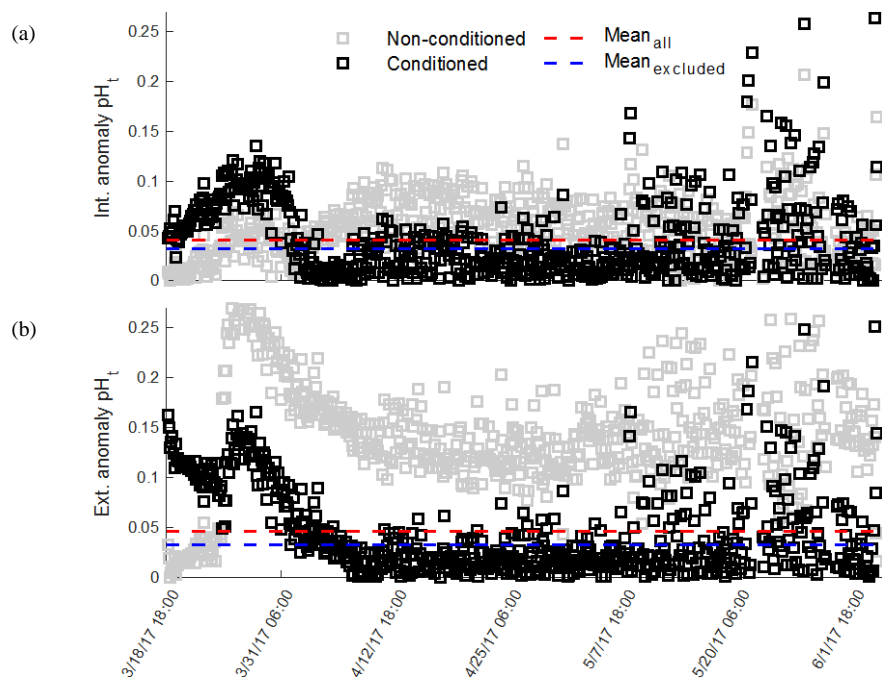


1120  
1121  
1122  
1123  
1124  
1125  
1126  
1127  
1128  
1129  
1130  
1131  
1132  
1133  
1134  
1135  
1136

Comparison of pH<sub>t</sub> recorded by the internal (panel a and b) and external (panel c and d) electrodes on conditioned SeaFET<sup>TM</sup><sub>395</sub> (blue) and SeaFET<sup>TM</sup><sub>396</sub> (purple) deployed in Kasitsna Bay, AK, based on calibration method: factory calibration (FC) and *in situ* single-point (SC) calibration. The data set here is the same as figure 4, but timing of calibration method is different. Discrete reference samples (black asterisks) and calibration sample (red asterisks) were collected < 24 h post deployment and 12 h pre-SeaFET<sup>TM</sup> recovery, while calibration sample was collected 36 h pre-SeaFET<sup>TM</sup> recovery. Temperature and salinity measurements collected on reference and calibration samples were used to derive SeaFET<sup>TM</sup> pH<sub>t</sub> at those given time points. All other SeaFET<sup>TM</sup> pH<sub>t</sub> measurements use thermistor temperature and salinity logged by Kasitsna Bay data sonde.

1137  
1138  
1139  
1140  
1141  
1142  
1143

Figure 6.

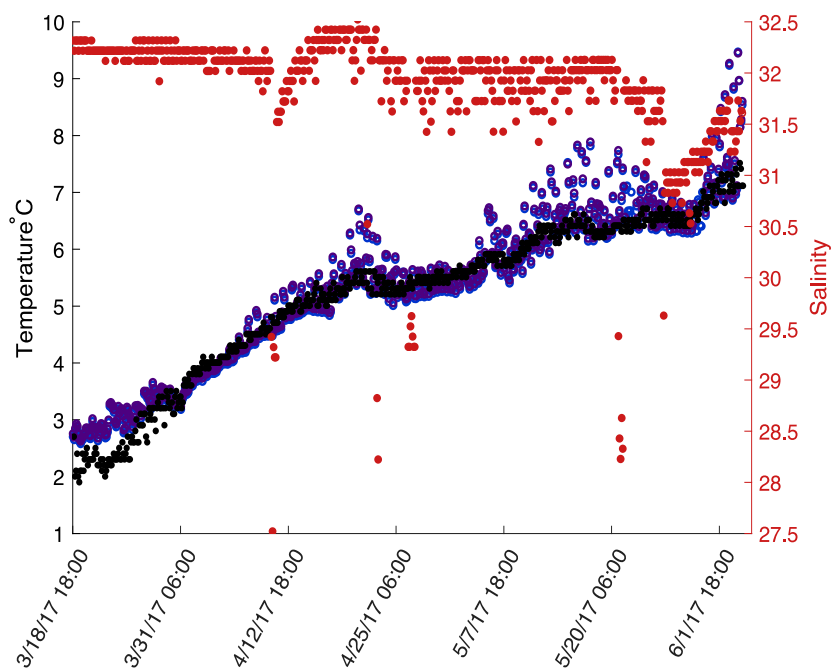


1144  
1145  
1146  
1147  
1148  
1149  
1150  
1151  
1152  
1153  
1154  
1155  
1156  
1157  
1158  
1159  
1160

Mean pH<sub>t</sub> anomaly between *in situ* single-point calibrated SeaFET<sup>TM</sup><sub>395</sub> and SeaFET<sup>TM</sup><sub>396</sub> internal (panel a) and external (panel b) electrodes during parallel deployment in Kasitsna Bay, AK. Intra-anomaly comparison based on calibration sample taken at initial deployment (< 24 h non-conditioned, gray squares) and end of deployment (36 h pre-recovery, black squares). Shaded blue region indicates conditioning period. Data points in blue region omitted when mean anomaly was calculated (non-conditioned: transparent blue-dashed line; conditioned: bold blue-dashed line) compared to mean anomaly from entire data set (non-conditioned to environment: red-dashed line; conditioned: red-dashed line).

1161  
1162  
1163  
1164  
1165  
1166  
1167

Figure 7.



1168  
1169  
1170  
1171  
1172  
1173  
1174  
1175  
1176  
1177  
1178  
1179  
1180  
1181  
1182  
1183  
1184

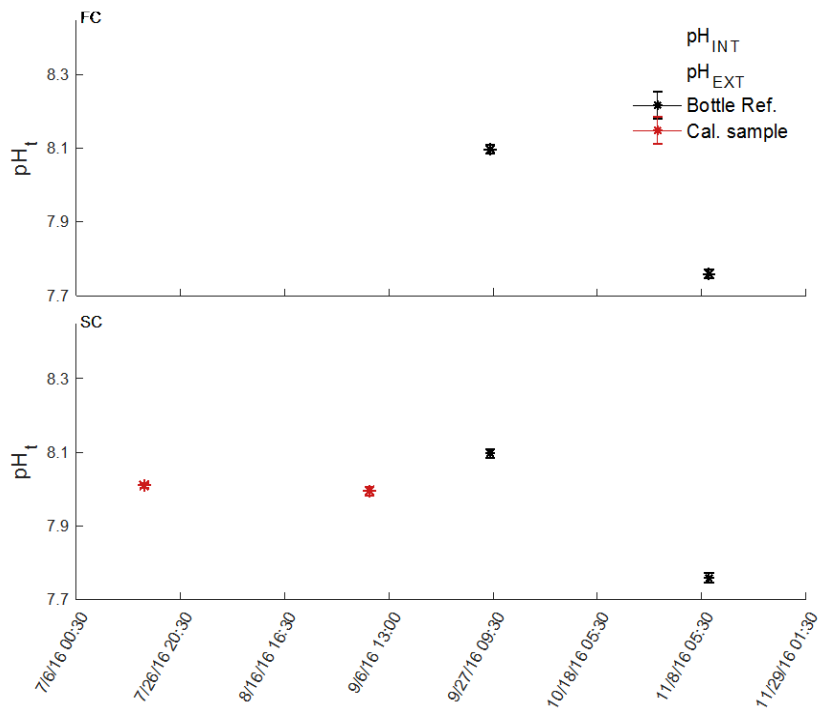
Temperature derived from the internal thermistor on SeaFET<sup>TM</sup><sub>395</sub> (blue) and SeaFET<sup>TM</sup><sub>396</sub> (purple) compared against the temperature recorded by the Kachemak Bay National Estuarine Research Reserve data sonde. Salinity (Red circles) recorded by Kachemak Bay data sonde on the right y-axis.

1185  
1186  
1187  
1188  
1189  
1190  
1191

Figure 8.

(a)

(b)

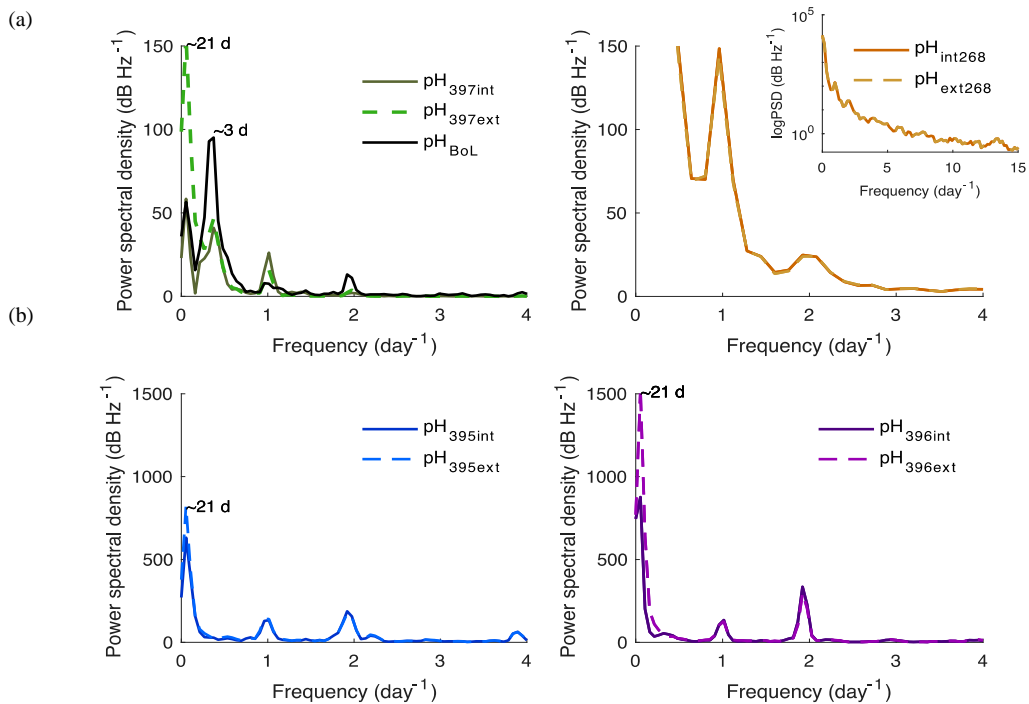


1192  
1193

1194  $pH_t$  recorded by the internal (solid) and external (dashed) electrodes on SeaFET<sup>TM</sup><sub>268</sub> deployed at  
 1195 the Sentry Shoal mooring.  $pH_t$  from both electrodes is shown when derived using factory  
 1196 calibration (FC) coefficients (panel a) and *in situ* single-point (SC) calibration coefficients (panel  
 1197 b). Black asterisks are references samples taken after initial calibration and recalibration (red  
 1198 asterisk), where  $pH_t$  was derived from  $TCO_2$  and  $pCO_2$  measurements made on the BoL at the  
 1199 Hakai Institute's Quadra Island Field Station.

1200  
1201  
1202  
1203  
1204  
1205  
1206  
1207  
1208  
1209  
1210  
1211  
1212  
1213  
1214  
1215

**Figure 9.**

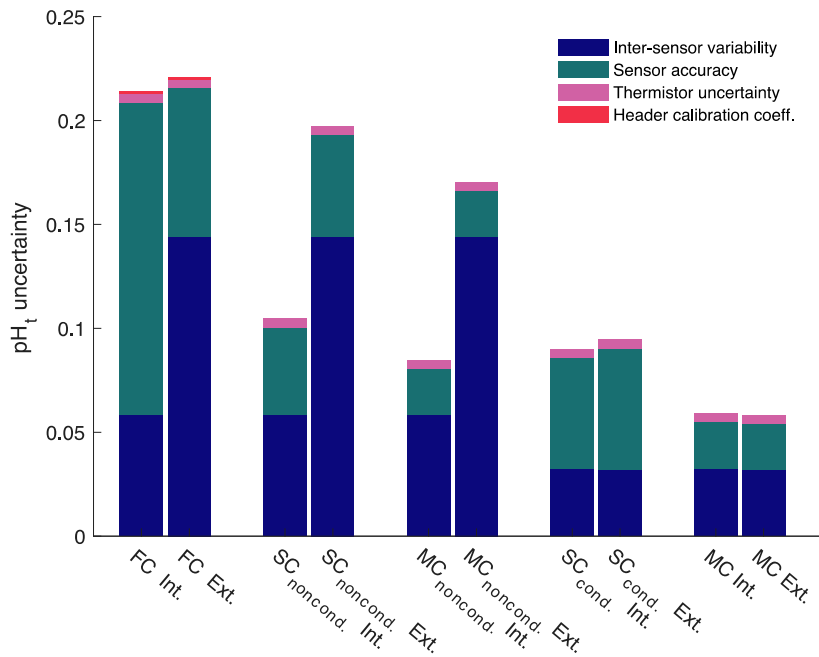


1216



1217  
 1218 Power spectral density (PSD) analysis of  $pH_t$  in frequency per day for SeaFETs™ 397 (panel a),  
 1219 268 (panel b), 395 (panel c), and 396 (panel c). Inset in panel b is log base 10 transformed PSD  
 1220 analysis of same data set. All internal electrodes marked as solid colored lines while external  
 1221 electrodes are colored dashed lines. BoL data set marked as solid black line (panel a).  
 1222  
 1223  
 1224  
 1225  
 1226  
 1227  
 1228  
 1229  
 1230  
 1231  
 1232  
 1233  
 1234  
 1235  
 1236  
 1237  
 1238

**Figure 10**



1239  
 1240

1241 Quantified uncertainties based on field deployments of all Sea-Bird SeaFETs™ separated by  
1242 electrode calibration method (FC: factory; SC: single-point; MC: multi-point), and calibration  
1243 time for SeaFETs™ 395 and 396 (i.e., non-conditioned to environment and conditioned). pH<sub>t</sub>  
1244 accuracy uncertainty calculated as the mean difference when comparing the absolute difference  
1245 between reference samples and SeaFETs™ 395 (non-conditioned to environment and  
1246 conditioned), 396 (non-conditioned to environment and conditioned), and 268 as well as the  
1247 average absolute difference between SeaFET™ 397 and the BoL. Inter-sensor variability  
1248 uncertainty determined by comparing SeaFETs™ 395 (non-conditioned to environment and  
1249 conditioned) and 396 (non-conditioned to environment and conditioned), deployed side-by-side  
1250 in Kasitsna Bay. Thermistor uncertainty is calculated pH<sub>t</sub> error when using thermistor derived  
1251 temperature rather than external temperature sensor determined from SeaFETs™ 395 and 396.  
1252 Header calibration coefficient uncertainty is the discrepancy in pH<sub>t</sub> when using SeaFETcom  
1253 factory calibration coefficients from header file rather than disc file.  
1254  
1255